



Review

S-N Curve Models for Composite Materials Characterisation: An Evaluative Review

Ibrahim Burhan and Ho Sung Kim *

Mechanical Engineering, School of Engineering, Faculty of Engineering and Built Environment, The University of Newcastle, Callaghan, NSW 2308, Australia; Ibrahim.Burhan@uon.edu.au

* Correspondence: ho-sung.kim@newcastle.edu.au; Tel.: +61-2-4921-6211

Received: 24 May 2018; Accepted: 25 June 2018; Published: 2 July 2018



Abstract: S-N behavior has been a backbone of material fatigue life studies since the 19th century. Numerous S-N curve models have been produced but they have been arbitrarily chosen in numerous research works dominantly for composite materials. In this paper, they were critically reviewed and evaluated for capability using the following criteria: data fitting capability, efficiency of curve fitting, applicability to data sets at various stress ratios (-0.43 , -1 , -3 , 0.1 , and 10), representability of fatigue damage at failure, and satisfaction of the initial boundary condition. The S-N curve models were found to be in two categories—one for fatigue data characterization independent of stress ratio, and the other for those designed for predicting the effect of stress ratio. The models proposed by Weibull, Sendeckyj, and Kim and Zhang for fatigue data characterization appeared to have the best capabilities for experimental data obtained from Weibull for $R = -1$, from Sendeckyj for $R = 0.1$, and from Kawai and Itoh (for $R = -0.43$, -3 , and 10). The Kim and Zhang model was found to have an advantage over the Weibull and the Sendeckyj models for representing the fatigue damage at failure. The Kohout and Vechet model was also found to have a good fitting capability but with an inherent limitation for shaping the S-N curve at some stress ratios (e.g., $R = -0.43$). The S-N curve models developed for predicting the effect of stress ratio were found to be relatively inferior in data fitting capability to those developed directly for fatigue data characterization.

Keywords: S-N curve; model; curve fitting capability; curve fitting efficiency; fatigue damage; stress ratio

1. Introduction

Fatigue is a phenomenon that causes the progressive damage to materials under cyclic loading. The damage physically consists of cracks and deformation. It eventually leads to the final failure of materials. There have been two different ways to approach the fatigue damage. One of the ways is to deal with cracks individually using fracture mechanics parameters such as the stress intensity factor [1]. The other way is to deal with relatively “small” cracks [2] for fatigue life in a collective manner including crack initiation at a relatively large scale of un-notched geometry with respect to the initial flaws, which requires an S-N curve model for characterization. (S and N in the acronym stand for stress and number of fatigue loading cycles at failure respectively.) Some S-N curve models have been derived from fatigue damage formulations while some others are intuitively obtained empirically or statistically using the Weibull distribution [3]. The S-N curve models have been used for both monolithic and composite materials. The difference between the two types of materials in S-N curve modelling has not significantly been found although the fatigue damage growth pattern varies dependent on material structure. Small cracks, for example, grow in polymeric matrix in the case of fiber reinforced composites but a follow-up crack propagation stage leading to the final failure (or complete separation into two pieces) is often not clearly defined [4–6] whereas the initiation site(s)

and crack propagation traces in the case of monolithic materials are usually identifiable on the fracture surfaces [7–9].

An S-N curve is essential not only for characterizing fatigue test results from un-notched specimens but also for the remaining fatigue life predictions involving fatigue damage quantification and stress ratio effect. Thus, the S-N curve behavior has been a backbone of fatigue life studies since the 19th century. A historian refers to the fatigue test results published in 1837 by Albert [10] and to the term “fatigue” appeared in 1854 [11] as the first ones. Some early fatigue studies, in fact, had begun without an S-N curve model [12]. Also, the S-N fatigue study development in history has been somewhat disorderly in sequence of events, slowing down the knowledge advancement. For example, the research of stress ratio effect on fatigue life [13–16]) mostly appears earlier than S-N curve modelling [17–20] although S-N curve modelling should be a prior task to the stress ratio effect for fatigue life prediction. One would be surprised to find the fact that the stress ratio effect has still been a contemporary research topic [21,22] since the 19th century. On the other hand, the study on fatigue damage [23–27] for fatigue life prediction seems to be concurrent with modelling of S-N curve [20,21].

A primary reason for the slow progress in S-N fatigue life prediction studies despite the long history may be that the studies on other topics such as stress ratio effect and fatigue damage for fatigue life predictions cannot be efficiently conducted without knowing an adequate deterministic S-N curve model. Other reasons may be as follows: (a) researchers have been persistent in adhering to particular S-N curve model(s) or producing their own model(s) regardless of the benefits of existing models [20,22,24]; and (b) researchers tend to choose particular damage accumulation rules which are not necessarily valid [28]. Palmgren and Miner’s model [23,29] may be one of those chosen by many researchers even though the Palmgren and Miner damage model is not accurate as Schutz [10] in his historical review pointed out. Also, evidence for the slow progress has been found in the literature. Philippidis and Passipoularidi [30] evaluated nine selected damage models involving residual strength degradation in relation to fatigue life. They found that no model is consistent in accurately predicting the residual strength degradation behavior of different composite laminates for fatigue life. Post et al. [31] also selectively evaluated twelve fatigue life prediction models for spectrum loading applications; they summarized that most of the investigators who proposed models simply fit them to their experimental results with their predictive ability remaining uncertain. It is only recently that Eskandari and Kim [27,32] returned to the fundamentals and provided mathematical reasoning for how fatigue damage models in the past went invalid for predicting the remaining fatigue life. Also, it is true that some researchers [33] still concurrently pursue the conventional approach based on the Palmgren and Miner’s damage model [23,29] without the fundamental basis.

Some literature dealing with S-N curve models has been available since Weibull [34] discussed S-N curve models. Schutz [10] discussed the Basquin model [17] within the context of fatigue history for a period of 1838–1996. Kohout and Vechet [35] reviewed a few S-N curve models in relation to a newly proposed model. Some S-N curve models were overviewed by Nijssen [36]. Recently, Xiong and Shenoi [37] listed four S-N curve models including Basquin model as the generally accepted ones in a monograph. However, the capabilities of S-N curve models for applications at different stress ratios have been neither much known nor extensively reviewed.

In this paper, S-N curve models available since 1910 are critically reviewed and evaluated to identify their capabilities for applications at a wide range of stress ratios when subjected to the uniaxial loading for less than giga load cycles which may be more applicable for composite materials. For evaluation and critical review, the following criteria were adopted: capability of curve fitting, efficiency of curve fitting, applicability to data sets at various stress ratios, representability of fatigue damage at failure, and satisfaction of S-N curve initial boundary condition at the first load cycle.

2. Criteria for S-N Curve Model Evaluation

An S-N curve model is a line shape function preferably on a log-log or lin-log scale for representing the phenomenon of fatigue life dependent on fatigue damage. For evaluation of, and

critical review on, S-N curve models, the following criteria may be considered [38]: (a) capability of curve fitting, (b) efficiency of fitting parameter determination, (c) adaptability to various stress ratios, (d) representability of fatigue damage at failure, and (e) satisfaction of the initial boundary condition of S-N curve at the first load cycle. These criteria may be useful for evaluation as will be detailed.

Capability of curve fitting may be the most important criterion because the purpose of any S-N curve, in the first instance, is to characterize the fatigue test data prior to predicting fatigue lives under various conditions. The capability is virtually for curve shaping, complying with the data trend. Once capability of curve fitting is sufficient, an efficiency of fitting parameter determination may be considered. The number of fitting parameters in a model may be judged for the efficiency. If the number of fitting parameters is two, parameters may typically be determined using the traditional least square methods for fitting data in log-log coordinates as for the Basquin model or they can be determined using the well-established statistical methods. However, more than two fitting parameters would inevitably lead to a low efficiency of determination, requiring an additional algorithm.

Adaptability to various stress ratios may be an important criterion for wider applications although most of S-N models have been developed for particular stress ratios. It is useful to deal with the complex fatigue loading involving random variation [39] and to eventually be developed in conjunction with fatigue damage for predicting the remaining fatigue life. As shown in Figure 1 for a stress amplitude (σ_a) vs mean stress (σ_{mean}) diagram, the stress ratios are divided into four ranges depending on loading type: $R = 0-1$ under tension-tension (T-T) loading, $R = 0--1$ under tension-compression (T-C) loading, $R = -1--\infty$ under compression-tension (C-T) loading, $R = -\infty-1$ under compression-compression (C-C) loading. The adaptability can be evaluated for capability of curve fitting by varying values of fitting parameters in S-N curve model at different stress ratios.

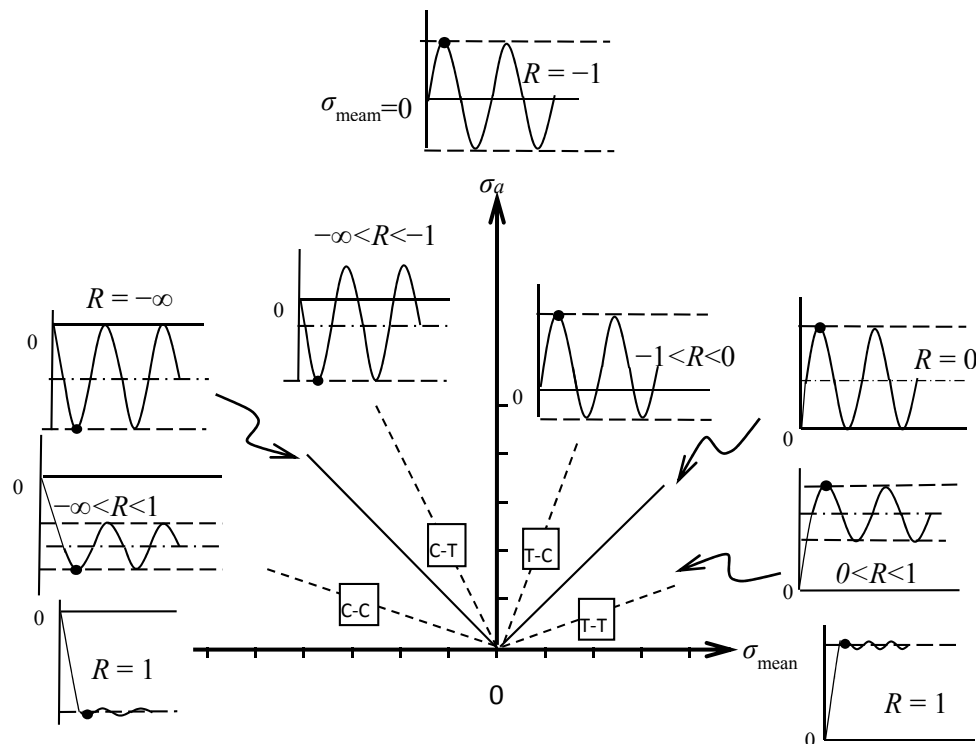


Figure 1. Stress ratio ranges on σ_a - σ_{mean} diagram for the loading types: T-T, T-C, C-T, and C-C.

Representability of fatigue damage at failure applies to some of S-N curve models derived from the fatigue damage formulations. The damage accumulated during cycling (D) or damage at failure (D_f) has existed confusingly in many different forms as listed by Hwang and Han [20], Fatemi and Yang [40], Yang and Fatemi [41], Bathias and Pineau [42], and Christian [43]. A clear difference, though,

between damage at failure (D_f) and damage prior to failure (D) should be made to clarify D_f [27]. Damage at failure (D_f) is directly related to an S-N curve which is a locus of failure points caused by damage. Thus, an S-N curve itself indicates damage at failure in a way. Other quantities such as residual strength and residual modulus [44] may be able to represent the damage as well. More importantly, however, if the ultimate purpose of damage D is to predict the remaining fatigue life when applied stress varies, a damage function (D), which is a function of N and applied peak stress σ_{max} , is required to satisfy the compatibility condition [27] to ensure that σ_{max} and N compatibly contribute to the damage. If an S-N curve is derived from fatigue damage and to predict the remaining fatigue life involving independent variables (i.e., N_f and σ_{max}), the damage at tensile failure D_{fT} is required to satisfy

$$\frac{\partial D_{fT}}{\partial \sigma_{max}} = -A \tag{1}$$

or, for damage at compressive failure D_{fC} ,

$$\frac{\partial D_{fC}}{\partial |\sigma_{min}|} = -A \tag{2}$$

where $A =$ a constant greater than zero.

Satisfaction of the initial boundary condition of S-N curve at the first load cycle is to ensure the correspondence with a static strength to cover a full range of applied stress levels in establishing a full S-N plane for fatigue damage determination. It is also a requirement for predicting the remaining fatigue life because the initial boundary condition affects the size of an S-N plane and subsequently the damage quantity [27]. The initial boundary condition, in fact, has been arbitrary as will be discussed. For example, some researchers have adopted $N_f = 0$ or 0.5 or 1 at σ_{uT} in the absence of a rigorous rational basis while some earlier researchers have ignored the initial boundary condition. Eskandari and Kim [27] recently provided a rationale for $R = 0$ to be $N_f = 0.5$ at σ_{uT} . However, it has not generally been settled down on other stress ratios yet. Nonetheless, it is necessary that N_f at σ_{uT} should be $0 < N_f < 1$ or adjustable for the future development until a rational value is found while $N_f = 0$ should not be used not only because it is physically impossible to be a failure point but also because it does not exist on log coordinate axis.

Finally, if an inverse expression of S-N curve equation is obtainable, it would be technically useful for converting between σ_{max} and N_f without a numerical scheme.

3. S-N Curve Models

3.1. For Fatigue Data Characterisation

S-N curve models developed directly for characterization of fatigue experimental data subjected to a constant amplitude of loading at a constant stress ratio (R) will be discussed in this section.

Some of early S-N curve models had been intuitively formulated. The Basquin model [17] may be the first among those:

$$\sigma_{max} = \alpha(N_f)^\beta \tag{3}$$

where σ_{max} = applied peak stress, α, β = model fitting parameter, and N_f = number of cycle at failure.

It represents a straight line in log-log coordinates. Equation (3) has been the most frequently used model [45] even though it does not fully fit the experimental data. It is problematic in some applications although the fitting parameters are easily determined. An alternative form to Equation (3) may be in a linear-log form given by;

$$\sigma_{max} = \alpha(\log N_f) + \beta \tag{4}$$

Subramanyan [46], Mandell and Meier [47], Bond and Farrow [48], and Tamuzs et al. [49] adopted this linear-log form for various stress ratios while Gathercole et al. [50], Adam et al. [51], and Beheshty et al. [52] adopted polynomial curve fitting of experimental data for σ_{\max} versus $\log N_f$.

Although the fatigue limit (σ_∞) may not exist [53], Stromeyer [54] added an additional term, σ_∞ , to Equation (3):

$$\sigma_{\max} = \alpha(N_f)^\beta + \sigma_\infty \tag{5}$$

where σ_{\max} = applied peak stress, α, β = model fitting parameter, and N_f = number of cycle at failure.

Palmgren [23] added one more parameter to have,

$$\sigma_{\max} = \alpha(N_f)^\beta + \sigma_\infty \tag{6}$$

where σ_{\max} = applied peak stress, σ_∞ = fatigue limit, α, β, γ = model fitting parameter, N_f = number of cycle at failure, and δ = number of stress cycles to which the balls or the grooves are subjected during one revolution of the bearing.

Weibull [18] considered an equation for modification suggested by E. Epremian in a private communication;

$$\frac{\sigma_{\max} - \sigma_\infty}{\sigma_{uT} - \sigma_\infty} = 1 - \psi(\alpha \log N_f + \beta) \tag{7}$$

where σ_{\max} = applied peak stress, σ_{uT} = ultimate tensile strength, σ_∞ = fatigue limit, α, β = model fitting parameter, N_f = number of cycle at failure, and ψ = Gaussian error function, and subsequently proposed an S-N curve model;

$$\sigma_{\max} = (\sigma_{uT} - \sigma_\infty) \exp[-\alpha(\log N_f)^\beta] + \sigma_\infty \tag{8}$$

including both the ultimate strength (σ_{uT}) and the fatigue limit (σ_∞). The two fitting parameters (α and β) in Equation (8) can be determined by taking log on both sides of,

$$\frac{\sigma_{\max} - \sigma_\infty}{\sigma_{uT} - \sigma_\infty} = \exp[-\alpha(\log N_f)^\beta] \tag{9}$$

The Weibull model allows the initial boundary condition of the S-N curve to be $N_f = 1$ at $\sigma_{\max} = \sigma_{uT}$ and is efficient for determining the fitting parameters although the fatigue damage was not considered. The fatigue limit in the equation, which may not exist, is a disadvantage for curve fitting. However, the assumed fatigue limit may be regarded as being different from a fitting parameter because they can easily be estimated for fitting purposes whereas fitting parameters can be found on a trial and error basis in some cases without much idea on the initial trial value unless a known algorithm is available.

Henry and Dayton [55] assumed

$$\sigma_{\max} = \frac{\alpha}{N_f} + \beta \tag{10}$$

where σ_{\max} = applied peak stress, α, β = model fitting parameter, and N_f = number of cycle at failure, for an S-N curve to derive a “damage equation”, which is far from being accurate for data fitting although an initial boundary condition at the first load cycle can be managed to be met.

Sendeckyj [19] proposed

$$\sigma_{\max} = \frac{\sigma_{uT}}{(1 - \alpha + \alpha N_f)^\beta} \tag{11}$$

or

$$N_f = \frac{(\sigma_{uT}/\sigma_{\max})^{1/\beta} - 1 + \alpha}{\alpha} \tag{12}$$

where σ_{\max} = applied peak stress, σ_{uT} = ultimate tensile strength α, β = model fitting parameter, and N_f = number of cycle at failure.

Based on the assumption that so called “equivalent static strength” is of two-parameter Weibull distribution. A way of determination of parameters (α and β) was suggested to follow the steps: (a) estimation of initial α and β values using a computer program, (b) transformation of fatigue data using the estimated initial values into equivalent static strength data, and (c) fitting a Weibull distribution with a solution of non-linear algebraic equation. The steps (b) and (c) are repeated with renewed estimated values until the maximum-likelihood value of the shape parameter estimate is obtained. It is noted that this procedure needs a separate computing algorithm in addition to the first estimation for fitting parameter determination. Equations (11) and (12), however, are with only two fitting parameters so that they can be rapidly found without the procedure suggested by Sendeckyj.

Hwang and Han [24] formulated by defining so called “fatigue modulus” and a strain failure criterion:

$$N_f = \left[\alpha \left(1 - \frac{\sigma_{\max}}{\sigma_{uT}} \right) \right]^{1/\beta} \tag{13}$$

or

$$\sigma_{\max} = \sigma_{uT} \left(1 - \frac{N_f^\beta}{\alpha} \right) \tag{14}$$

where σ_{\max} = applied peak stress, σ_{uT} = ultimate tensile strength α , β = model fitting parameter, and N_f = number of cycle at failure.

The Hwang and Han model is based on the assumption that the fatigue modulus degradation rate follows a power function. Equations (13) and (14), however, do not satisfy an initial boundary condition, given that N_f should be zero for $\sigma_{\max} = \sigma_{uT}$, which is not possible on logarithmic coordinates used for N_f .

Ellyin in 1989 [56] proposed the total strain energy input (ΔW) as

$$\Delta W = \alpha' (N_f)^{\beta'} + C \tag{15}$$

where ΔW = total energy input, α' , β' = model fitting parameter, N_f = number of cycle at failure, and C = constant.

Subsequently, Ellyin and El-Kadi [57] adopted and converted this equation for a constant stress ratio with $C = 0$. They demonstrated that Equation (15) is consequently the same form as the Basquin model Equation (3).

Kensche [58] used the maximum strain (ϵ_{\max}) instead of the maximum stress for an S-N relation,

$$\epsilon_{\max} = \beta \frac{-\ln P(N_f)^{\frac{1}{\alpha}}}{[(N_f - \alpha')\gamma']^\gamma} \tag{16}$$

where α , β , γ' = shape and the scale parameters respectively for the Weibull distribution, and $P(N_f)$ = probability of survival.

The parameter γ' allows flattening or steepening of the curve, and $\alpha' = (1 - \gamma')/\gamma'$. This equation, in the first place, is not efficient for curve fitting because of the number of fitting parameters although it may be capable of curve fitting at different stress ratios as demonstrated in [58]. Also, it is not common to use the strain vs number of cycles (N_f) for fatigue characterization, unless other aspects are dealt with (e.g., thermos-mechanical fatigue in [59]), because the strain needs to be converted into stress for an S-N curve.

Kohout and Vechet [35] proposed a model to describe an assumed geometrical shape of the S-N curve

$$\sigma_{\max} = \sigma_\infty \left[\frac{(N_f + \alpha)}{(N_f + \gamma)} \right]^\beta = \sigma_{uT} \left[\frac{(1 + N_f/\alpha)}{(1 + N_f/\gamma)} \right]^\beta \tag{17}$$

or

$$\sigma_{\max} = \sigma_\infty \left[\frac{N_f}{(N_f + \gamma)} \right]^\beta \tag{18}$$

or

$$\sigma_{\max} = \sigma_{uT} \left[\frac{(N_f + \alpha)}{\alpha} \right]^\beta \tag{19}$$

where σ_{\max} = applied peak stress, σ_{uT} = ultimate tensile strength, σ_∞ = fatigue limit, α, β, γ = model fitting parameters, and N_f = number of cycle at failure.

Equation (17) is applicable for both low and high cycles, but Equation (18) is not applicable for high cycles. Equation (19) may be generally applicable without a known fatigue limit. Equations (17) and (18) extend the Basquin model to both the low-cycle and the assumed fatigue limit (σ_∞) regions while Equation (19) extends to the low-cycle region. The Kohout and Vechet model has generally three straight lines to describe the assumed S-N curve in log-log coordinates, including two asymptotes with zero slope for tensile strength and fatigue limit (σ_∞), and a tangent for the region described by the Basquin model. The points of intersection of the tangent with the two asymptotes occur at $N_f = \alpha$ and $N_f = \gamma$ in the case of Equations (17) and (18). Thus, the parameters α and γ are numbers of cycles at which the S-N curve bends at high and low stresses respectively, and β is the slope of the tangent between the two bends (α and γ) in log-log coordinates. Kohout and Vechet model, therefore, is limited to the predetermined S-N curve. If the bend at a high stress does not exist at some stress ratios, it would not fit experimental data. Also, Equation (19) does not satisfy the initial boundary condition given that N_f should be zero to be $\sigma_{\max} = \sigma_{uT}$.

To derive an S-N curve, Kim and Zhang [60] quantified the fatigue damage at tensile fatigue failure (D_{fT}), which satisfies Equation (1):

$$D_{fT} = 1 - \frac{\sigma_{\max}}{\sigma_{uT}} \tag{20}$$

and they found that a fatigue damage rate follows

$$\frac{\partial D_{fT}}{\partial N_f} = \alpha (\sigma_{\max})^\beta \tag{21}$$

where σ_{\max} = applied peak stress, σ_{uT} = ultimate tensile strength, α, β = model fitting parameters, and N_f = number of cycle at failure.

The number of cycles at failure (N_f) in this equation can be obtained by integration, yielding an S-N curve as a function of applied peak stress (σ_{\max}):

$$N_f = \frac{\sigma_{uT}^{-\beta}}{\alpha(\beta - 1)} \left[\left(\frac{\sigma_{\max}}{\sigma_{uT}} \right)^{1-\beta} - 1 \right] + N_0 \tag{22}$$

or

$$\sigma_{\max} = \sigma_{uT} \left(\frac{\alpha(\beta - 1)(N_f + N_0)}{\sigma_{uT}^{-\beta}} + 1 \right)^{\frac{1}{1-\beta}} \tag{23}$$

The term N_0 in the equation is to adjust the initial number of cycles for the first cycle failure point according to the quantized analysis—it is not possible to find it with the continuity concept of S-N curve [27]. For example, $N_0 = 0.5$ cycle at $\sigma_{\max} = \sigma_{uT}$ with $R = 0$. Thus, the Kim and Zhang model satisfies the initial boundary condition. The fitting parameters for S-N curve in Equations (22) and (23) are identical to those for damage rate with respect to N_f (Equation (21)), which is an advantage for understanding a relation between damage rate and S-N curve. The two parameters (α and β) in Equations (22) and (23) can be determined for a set of fatigue data, given that Equation (21) is numerically,

$$\frac{\Delta D_{f(i)}}{\Delta N_{f(i)}} \approx \alpha (\sigma_{\max(i)})^\beta \tag{24}$$

where subscript $i = 1, 2, 3, \dots$ for different stress levels ($\sigma_{\max(i)}$) at failure, $\Delta D_{f(i)} = D_{f(i-1)} - D_{f(i)}$ for $D_{f(i-1)} > D_{f(i)}$ or $|1 - \sigma_{\max(i-1)}/\sigma_{uT}| > |1 - \sigma_{\max(i)}/\sigma_{uT}|$, $\Delta N_{f(i)} = N_{f(i-1)} - N_{f(i)}$ for $N_{f(i-1)} > N_{f(i)}$, and $\sigma_{\max(i)} = (\sigma_{\max(i)} - \sigma_{\max(i-1)})/2$.

Two different ways may be considered for numerically calculating $\Delta D_{f(i)}/\Delta N_{f(i)}$ and the corresponding $\sigma_{\max(i)}$. One of the ways is to directly use experimental data points on an S-N plane by choosing a pair of close data points for each value. The other way is to draw the best fit line manually through S-N data points for digitization (<http://arohatgi.info/WebPlotDigitizer/app/>) and then collect a set of digitized points. Then, $\log(\Delta D_{f(i)}/\Delta N_{f(i)})$ is plotted as a function of $\log \sigma_{\max(i)}$ such that β is the slope and 10^α is an intercept. It is practically efficient with, if necessary, a minimal iteration for the best fit. Figure 2 shows the sequence for plotting the best fit S-N curve.

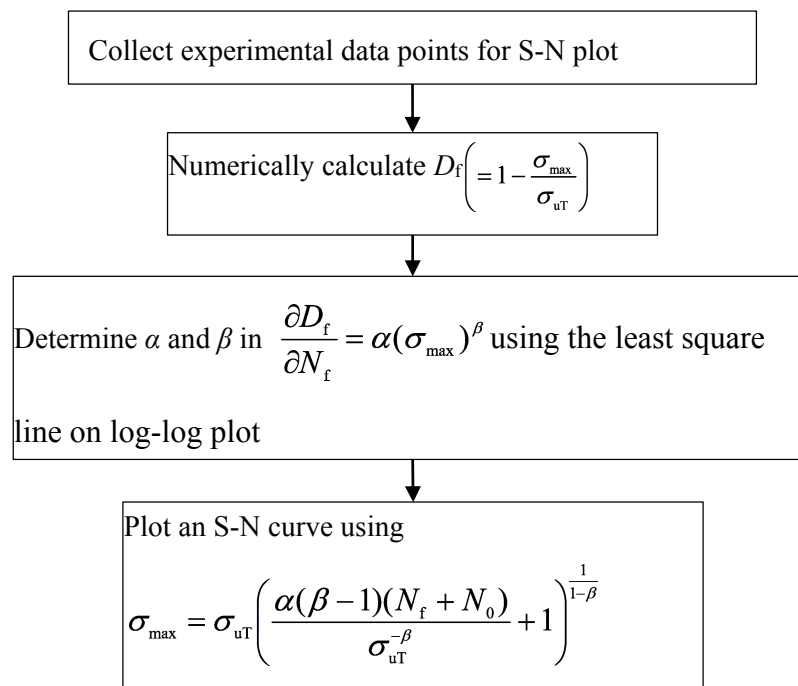


Figure 2. Sequence for plotting an S-N curve using the Kim and Zhang model.

Kassapoglou [61] statistically derived an S-N curve expression in a form same as Equation (3) for stress ratio (R) ranges, $0 \leq R \leq 1$ and $R > 1$, and another S-N curve expression for $R < 0$ but with more fitting parameters. Thus, Kassapoglou failed to model an S-N curve with one equation for application at different stress ratios. Nonetheless, further, Kassapoglou [62] replaced α in Equation (3) with static strength to have a static strength at $N_f = 1$ for predicting the remaining fatigue life under spectrum loading.

Kawai and Koizumi [21] assumed an S-N curve in conjunction with a constant fatigue life (CFL) diagram for stress ratio effect research:

$$2N_f = \frac{2}{\alpha} \frac{\left(1 - \frac{\sigma_{\max}^\chi}{\sigma_B}\right)^\beta}{\left(\frac{\sigma_{\max}^\chi}{\sigma_B}\right)^\gamma} \tag{25}$$

where $R = \chi = \sigma_{uC}/\sigma_{uT}$, and $\sigma_{\max}^\chi = \sigma_{\max}$ at χ .

This equation partially produces negative values for N_f as shown in Figure 3 with the values as used: $\alpha = 0.003$, $\beta = 1$, $\gamma = 8.5$, and $\sigma_B = (\sigma_{uT} + |\sigma_{uC}|)/2$. Thus, the fitting capability of this model is low. It has three fitting parameters (α , β , and γ) and one conditional property parameter (σ_B). In other words, if $\sigma_{uT} < |\sigma_{uC}|$ then $\sigma_B = \sigma_{uC}$; and if $\sigma_{uT} > |\sigma_{uC}|$ then $\sigma_B = \sigma_{uT}$. If a chosen value

in this way does not allow a good curve fitting, an alternative value σ_B between σ_{uT} and $|\sigma_{uC}|$ is required. Therefore, the efficiency of curve fitting for modelling is poor because of the number of fitting parameters and conditions imposed. The authors do not suggest a method of how to determine fitting parameters. Kawai and Itoh in 2014 suggested a similar S-N curve expression [22]:

$$2N_f = \frac{1}{\alpha} \frac{\langle 1 - \frac{\sigma_{max}^x}{\sigma_{uT}} \rangle^\beta}{\left(\frac{\sigma_{max}^x}{\sigma_{uT}}\right)^\gamma \langle \frac{\sigma_{max}^x}{\sigma_{uT}} - \frac{\sigma_{max}^L}{\sigma_{uT}} \rangle^\delta} \tag{26}$$

where σ_{max}^L = peak stress level at $R = -\infty$.

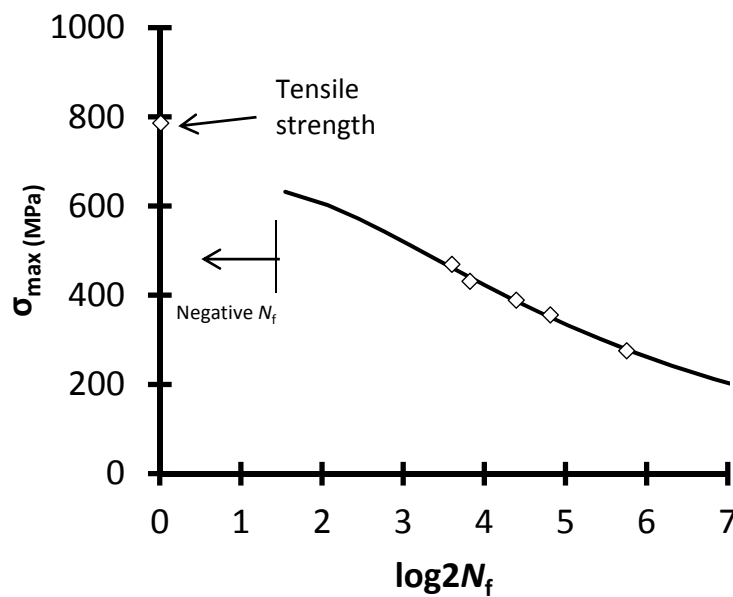


Figure 3. Experimental data from Kawai and Koizumi [21] for carbon fiber reinforced plastics with tensile strength = 782 MPa and compressive strength = 532 MPa obtained at $R = -0.68$. An S-N curve was fitted according to Equation (25) using $\alpha = 0.003$, $\beta = 1$, $\gamma = 8.5$, and $\sigma_B = (\sigma_{uT} + |\sigma_{uC}|)/2$.

The angular brackets $\langle \rangle$ denote the singular function (if it is negative, then zero to avoid negative number of cycles). It seems that they attempted to improve Equation (25) for S-N curve fitting but it cannot be used efficiently for the same reasons.

Major S-N curve models discussed in this section are listed in Table 1 and summarized with criteria for further discussion below.

3.2. As a Function of Stress Ratio

Some S-N curve models for stress ratio effect have been derived in relation to fatigue damage. One of reasons for this approach is that once fatigue damage is generally quantified, an S-N curve can possibly be found because S-N curve represents a special case of fatigue damage at failure as discussed above. Another reason is that the remaining fatigue life would be predictable if a valid damage function (D) is found. For these reasons, if damage is arbitrarily quantified, an S-N curve derived may not necessarily be capable of representing the fatigue data.

Table 1. Summary of selected S-N curve models for data characterization.

S-N Curve Models	Capability of Curve Fitting	Adaptability to Different Stress Ratios	Relation with Physical Properties			Remarks
			Boundary at Initial N_f	Damage Representation	Satisfaction of $\frac{\partial D}{\partial \sigma_{\max}} = -A$	
Basquin (1910)	Poor	Poor	N/A	N/A	N/A	
Stromeyer (1914)	Poor	Poor	N/A	N/A	N/A	
Weibull (1952)	Good	Good	Yes	N/A	N/A	Fatigue limit is required
Henry (1955)	Poor	N/A	N/A	N/A	N/A	
Marin (1962)	Poor	N/A	N/A	N/A	N/A	Same form as Basquin model.
Sendeckyj (1981)	Good	Good	Yes	N/A	N/A	
Hwang and Han (1986)	Poor	Poor	No	N/A	N/A	
Kohout and Vechet (2001) Equation (19)	Good	Good	No	N/A	N/A	With limited curve shaping (e.g., $R = -0.43$)
Kim and Zhang (2001)	Good	Good	Yes	Yes	Yes	

Poursartip et al. [25] defined a delamination damage of laminated composites as delaminated area divided by the total interfacial area, and subsequently determined the damage at failure (D_f) for a carbon fiber reinforced laminate made of 8 plies [45/90/-45/0/0/-45/90/45] with an average tensile strength of 586 MPa:

$$D_f = 2.857 \left(1 - \frac{\sigma_{\max}}{\sigma_{uT}} \right) \tag{27}$$

where σ_{\max} = applied peak stress, and σ_{uT} = ultimate tensile strength.

Equation (27) satisfies Equation (1) which is one of damage validity conditions. Further, they measured the stiffness reduction rate at $R = 0.1$ and calculated dD/dN by fitting the least square line to be

$$\frac{dD}{dN} = 9.189 \times 10^{-5} \left(\frac{\Delta\sigma}{\sigma_{uT}} \right)^{6.393} \tag{28}$$

where $\Delta\sigma$ = applied stress range, σ_{uT} = ultimate tensile strength, and N = Number of cycles before failure.

(Please note that D here is not at the failure.) Equation (28) could have been more useful for characterizing damage on the S-N plane if they found a valid function of D , but it is only for the linear part of experimental stiffness reduction-cycle curves. Also, it did not consider the compatibility conditions for fatigue damage (D) [27]. Poursatip and Beaumont [26] subsequently proposed an S-N curve for stress ratio (R) effect based on an empiricism with Equation (28),

$$N_f = 3.108 \times 10^4 \left(\frac{\sigma_{\max}(1-R)}{\sigma_{uT}} \right)^{-6.393} \left(1.222 \frac{1-R}{1+R} \right)^\gamma \left(1 - \frac{\sigma_{\max}}{\sigma_{uT}} \right) \tag{29}$$

where σ_{\max} = applied peak stress, σ_{uT} = ultimate tensile strength, γ = fitting parameter, N_f = number of cycle at failure, and R = stress ratio.

Equation (29) can be simplified by converting R into a constant for evaluating S-N curve performance,

$$N_f = \alpha \left(\frac{\sigma_{\max}}{\sigma_{uT}} \right)^{-6.393} \left(\frac{\sigma_{uT} - \sigma_{\max}}{\sigma_{uT}} \right) \tag{30}$$

The fitting parameter α in Equation (29) does not seem to be clearly linked to the damage rate in Equation (28) although the value 6.393 in Equation (30) indicates some correspondence. Also,

Equation (30) has only one fitting parameter so that it may be efficient for parameter determination if it fits data well.

Some S-N curve models simply assumed a residual strength function as the fatigue damage (D) while the prediction of the residual strength had been a single research topic by many researchers for fatigue damage [48,63–66]. D’Amore et al. [67] surmised a power law equation for a change rate of residual strength with respect to number of cycles for calculation and it was simply regarded as being identical to,

$$\frac{dD}{dN} = \alpha N^{-\beta} \tag{31}$$

where α, β = model fitting parameters, and N = number of cycle before failure.

The validity of Equation (31) is not known. It was followed by incorporating the stress ratio (R) with another surmise that one of the constants for the change rate of residual strength with respect to N is proportional to $\Delta\sigma$ to have:

$$N_f = \left[1 + \frac{1}{\alpha(1-R)} \left(\frac{\sigma_{uT}}{\sigma_{max}} - 1 \right) \right]^{1/\beta} \tag{32}$$

or

$$\sigma_{max} = \frac{\sigma_{uT}}{\alpha(N_f^\beta - 1)(1-R) + 1} \tag{33}$$

where σ_{max} = applied peak stress, σ_{uT} = ultimate tensile strength, N_f = number of cycle at failure, and R = stress ratio.

Taking R as a constant for S-N curve performance, we have

$$N_f = \left[\frac{\sigma_{uT} - \sigma_{max}}{\alpha' \sigma_{max}} + 1 \right]^{1/\beta} \tag{34}$$

where σ_{max} = applied peak stress, σ_{uT} = ultimate tensile strength, α', β = model fitting parameters, and N_f = number of cycle at failure.

A value given by $(\sigma_{uT}/\sigma_{max} - 1)/(1 - R)$ in Equation (32) was experimentally found to be constant for $R = 0.1-0.7$, allowing us to determine α and β ratios using data sets from different stress ratios. For a constant stress ratio, two fitting parameters need to be determined for an S-N curve. Caprino and Giorlea in 1999 [68] further experimentally verified this for $R = 10$ and 1.43 . Equation (34) allows the initial boundary condition to be $N_f = 1$ at σ_{uT} and the fitting parameters have a relation with Equation (31) for damage.

Epaarachchi and Clausen [69] followed an approach similar to that of D’Amore et al. [67]. They used Equation (31) to propose an S-N curve model not only as a function of stress ratio but also as a function of loading frequency (and fiber orientation angle of composites):

$$\sigma_{uT} - \sigma_{max} = \alpha \left(\frac{\sigma_{max}}{\sigma_{uT}} \right)^{0.6} \sigma_{max} (1-R)^{1.6} \frac{1}{f^\beta} (N_f^\beta - 1) \tag{35}$$

where σ_{max} = applied peak stress, σ_{uT} = ultimate tensile strength, α, β = model fitting parameters, f = loading frequency, N_f = number of cycle at failure, and R = stress ratio.

If this equation is simplified for S-N curve performance, it becomes

$$N_f = \left(\frac{\sigma_{uT} - \sigma_{max}}{\alpha' (\sigma_{max})^{1.6}} + 1 \right)^{1/\beta} \tag{36}$$

where α' = model fitting parameter, which is not much different from D’Amore model Equation (34). The only difference from Equation (34) is in an exponent 1.6. Later, Epaarachchi [70] demonstrated that

the model Equation (35) proposed by Epaarachchi and Clausen is not much capable of predicting S-N curve at high stress ratios unless so called “fatigue-static-fatigue curve” algorithm is used for fitting.

3.3. Associated with Stress Intensity Factor

Wyzgoski and Novak [71] attempted to relate the S-N curve with the initial and final flaw sizes using the Paris equation [72] given by

$$\frac{da}{dN} = A(\Delta K)^m \tag{37}$$

where ΔK = stress intensity factor range ($=Y\Delta\sigma a^{1/2}$), and A and m = constants.

They integrated this equation with limits for the final crack length (a_f) and initial crack length (a_0) assuming that geometry factor Y is constant:

$$N_f = \frac{2}{(m-2)AY^m(\Delta\sigma)^m} \left(\frac{1}{a_0^{\frac{(m-2)}{2}}} - \frac{1}{a_f^{\frac{(m-2)}{2}}} \right) \tag{38}$$

where $\Delta\sigma$ = stress range.

To improve the predictability of Equation (38), Wyzgoski and Novak [73] further adopted a relation between a_f and a_0 with $a_f = a_0$ for the first cycle fracture and $a_f = t$ for a low stress fracture:

$$a_f = t \exp \left[-\frac{\ln(t) - \ln(a_0)}{\sigma_{uT}} \frac{\Delta\sigma}{1-R} \right] \tag{39}$$

where R = stress ratio.

Please note that they eliminated a_f in Equation (38) for Equation (39). The initial crack length (a_0) in Equation (38) was regarded as a constant independent of applied stress level. The initial crack length a_0 may not be conceptually applicable for continuous fiber reinforced composites with a multiple crack damage pattern. However, the initial crack length (a_0) may be regarded as an equivalent initial crack to the damage consisting of multiple cracks, given that the S-N curve behavior pattern may be for both single and multiple crack damages for un-notched specimens. The Wyzgoski and Novak model may be useful for providing an insight into internal damage and understanding S-N curve in relation to the stress intensity factor. At the same time, it should be noted that the stress intensity factor is limited to the tensile stress, implying that applicability of this model is not certain for stress ratios involving compressive stress, and may not be practical for S-N curve fitting due to the number of fitting parameters if A and m are treated as the fitting parameters. Figure 4 shows experimental data for injection molded PBT reinforced with 30w% short glass fibers [73] (obtained at $R = 0.1$ with $\sigma_{uT} = 100$ MPa, specimen thickness (t) = 0.0032 m) in comparison with an S-N curve plotted in dashed line using Equation (38) for: Paris equation constants $A = 1.53 \times 10^{-10}$ and $m = 7.41$, geometry factor $Y = 1.17$ for a semi-circular surface flaw [74], initial flaw size (a_0) = 0.354 mm. Also, another S-N curve plotted with Kim and Zhang model Equation (22) or (23) with $\alpha = 4.9 \times 10^{-35}$ and $\beta = 15.028$ is shown in solid line. The Wyzgoski and Novak model appear reasonable for curve fitting although it is not as accurate as the Kim and Zhang model (see below for capability).

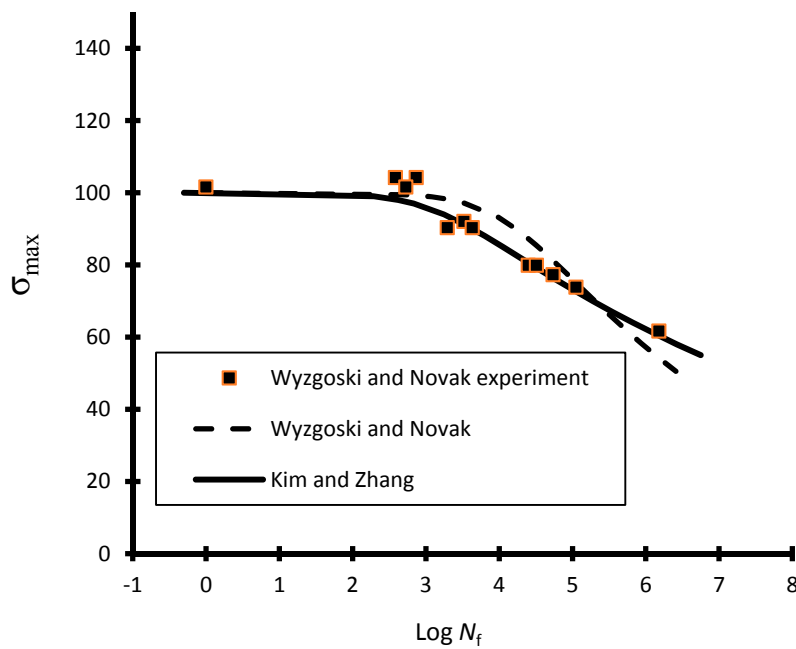


Figure 4. Wyzgoski and Novak [71] experimental data and S-N curve according to Equation (38) with $t = 0.0032$ m, $m = 7.41$, $A = 1.53 \times 10^{-10}$ m/cycle, $Y = 1.17$, $R = 0.1$, and $a_0 = 0.354$ mm. Another S-N curve was plotted according to the Kim and Zhang model Equation (23) with $\alpha = 1.53 \times 10^{-10}$ and $\alpha = 15.028$.

4. Evaluation of S-N Curve Model Capability

Experimental data obtained at five different stress ratios i.e., $R = -1, 0.1, -0.43, -3$, and 10 , which are available in the literature, will be used for S-N curve fitting evaluation. The stress ratio $R = -1$ was obtained from the rotating beam test which is readily implementable compared to other stress ratios to represent the loading between T-C and C-T (Figure 1). The other stress ratios: $R = 0.1$ may represent the tension-tension (T-T) loading for a range $R = 0-1$; $R = -0.43$ the tension-compression (T-C) loading for range $R = 0--1$; $R = -3$ the compression-tension (C-T) loading for a range $R = -1--\infty$; and $R = 10$ the compression-compression (C-C) loading for a range $R = -\infty-1$. When an S-N curve model involves compressive stress and failure, σ_{max} will be replaced with $|\sigma_{min}|$, and σ_{uT} with $|\sigma_{uC}|$ for evaluation.

4.1. S-N Curve Models for Data Characterisation

S-N curve models with more than two fitting parameters were eliminated from evaluation because its implementation is not economical, involving unnecessary efforts, given that some models available with two parameters are sufficiently accurate for data fitting. Some other models, fitting capabilities of which are poor due to the obvious limitation for curve shaping, were also eliminated from evaluation. For example, S-N curve models represented by Equations (4) and (5) are not much different from Basquin model Equation (3). Experimental data and plots will be in log-log coordinates, which are convenient for the Kohout and Vechet model Equation (19) in comparing with other models. Equations (17) and (18) were not employed here because they contain three fitting parameters with a fatigue limit.

An experimental data set for Bofors FR 76 Steel with $\sigma_{uT} = 829$ MPa obtained from Weibull [18] with 111 rotating beam tests at $R = -1$ is plotted in Figure 5 with data points having a probability of 50% failure. Two curves from the Weibull model Equation (8) with and without fatigue limit (σ_∞) for respective two sets of fitting values— $\alpha = 21 \times 10^{-4}$ and $\beta = 3.8$ with an assumed $\sigma_\infty = 353$ MPa (provided by Weibull), and $\alpha = 0.003$ and $\beta = 3.1$ with an assumed $\sigma_\infty = 0$ (to see if there would be any difference)—are plotted in comparison with other S-N models to be discussed. (Please note that the plotted lines from some of models are overlapped and therefore not clearly distinguishable.) The

capability of fitting with a fatigue limit (σ_∞) appears to be very good but, with $\sigma_\infty = 0$, it is relatively poor at a high N_f . The best fit with the fatigue limit by Weibull model may be regarded as the reference for comparisons with other S-N curves. Plots generated by other S-N models are shown with: $\alpha = 0.001$ and $\beta = 0.093$ for Sendeckyj model Equations (11) and (12); $\alpha = 35$ and $\beta = 0.21$ for Hwang and Han model Equations (13) and (14); $\alpha = 776.25$ and $\beta = -0.0895$ for Kohout and Vechet model Equation (19); and $\alpha = 10^{-38.44}$ and $\beta = 11.809$ for Kim and Zhang model Equations (22) and (23) with $N_0 = 0.5$. The fitting capabilities for models by Weibull, Sendeckyj, Kohout and Vechet, and Kim and Zhang appear to be practically identical to each other and may be regarded as being sufficiently good for practical data characterization. In contrast, the fitting capability of Basquin model Equation (3) is found to be poor as expected when σ_{uT} is included in data despite the fact that it has still been used by many researchers (e.g., refs. [75–77] to name a few). The fitting capability of Hwang and Han model appears to be also poor because of its limited capability—as the α value increases in Equations (13) and (14), σ_{max} approaches the ultimate strength at $N_f = 1$ but other part of the curve was found to deviate increasingly from the experimental data. A reasonable fit of Hwang and Han model can only be achieved by omitting the data points near the ultimate strength. The Basquin, and Hwang and Han models were accordingly eliminated from further comparison with other models at other stress ratios.

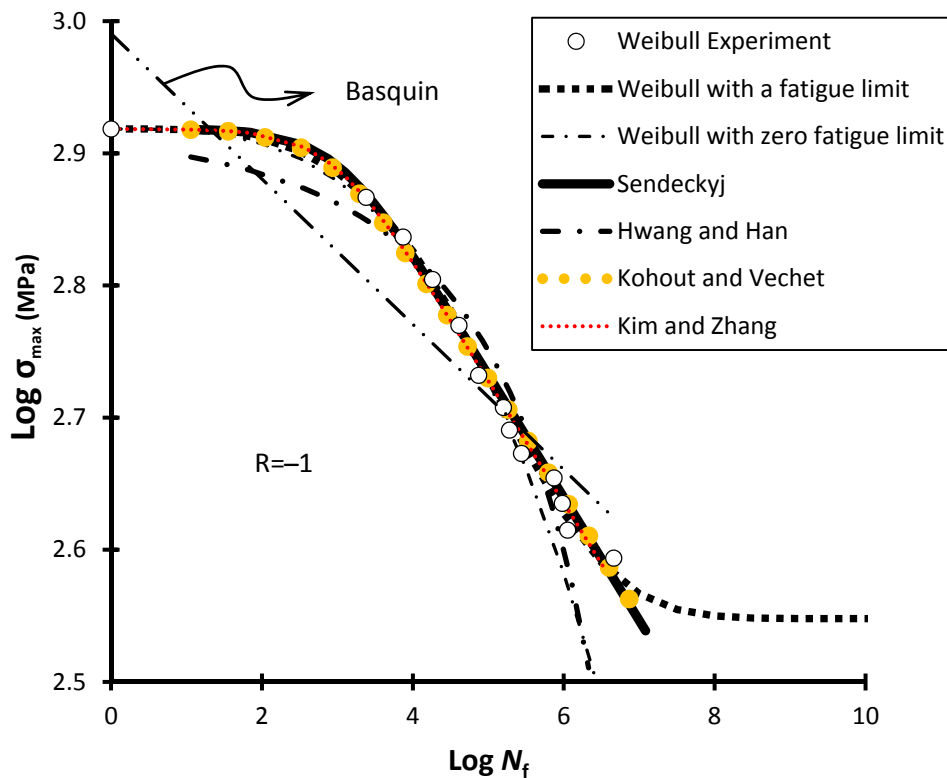


Figure 5. Weibull experimental data for $R = -1$ plotted with data points having a probability of 50% failure for Bofors FR 76 Steel rotating beam test with $\sigma_{uT} = 829$ MPa [18]. S-N curves were obtained from Weibull model with $\alpha = 21 \times 10^{-4}$ and $\beta = 3.8$ for an assumed $\sigma_\infty = 353$ MPa; Weibull model with $\alpha = 0.003$ and $\beta = 3.1$ for an assumed $\sigma_\infty = 0$; Sendeckyj model with $\alpha = 0.001$ and $\beta = 0.093$; Hwang and Han model with $\alpha = 35$ and $\beta = 0.21$; Kohout and Vechet model with $\alpha = 776.25$ and $\beta = -0.0895$; and Kim and Zhang model with $\alpha = 10^{-38.44}$, $\beta = 11.809$ and $N_0 = 0.5$.

For T-T loading at $R = 0.1$, an experimental data set consisting of 28 data points obtained from Sendeckyj [19] for glass fiber reinforced epoxy composite with $\sigma_{uT} = 2013$ MPa is given in Figure 6. Weibull model Equation (8) was plotted with $\alpha = 0.088$ and $\beta = 1.9$ for an assumed fatigue limit of 250 MPa, Sendeckyj model Equations (11) and (12) with $\alpha = 0.0485$ and $\beta = 0.157$, Kohout and Vechet

model Equation (19) with $\alpha = 19.953$ and $\beta = -0.155$, and Kim and Zhang model Equations (22) and (23) with $\alpha = 3.13 \times 10^{-27}$ and $\beta = 7.381$ for $N_0 = 0.5$. The S-N curve of Sendeckyj model may be regarded as the best fit as already demonstrated in [19]. The fitting capabilities of the four models still appear to be equally good and practically identical to each other.

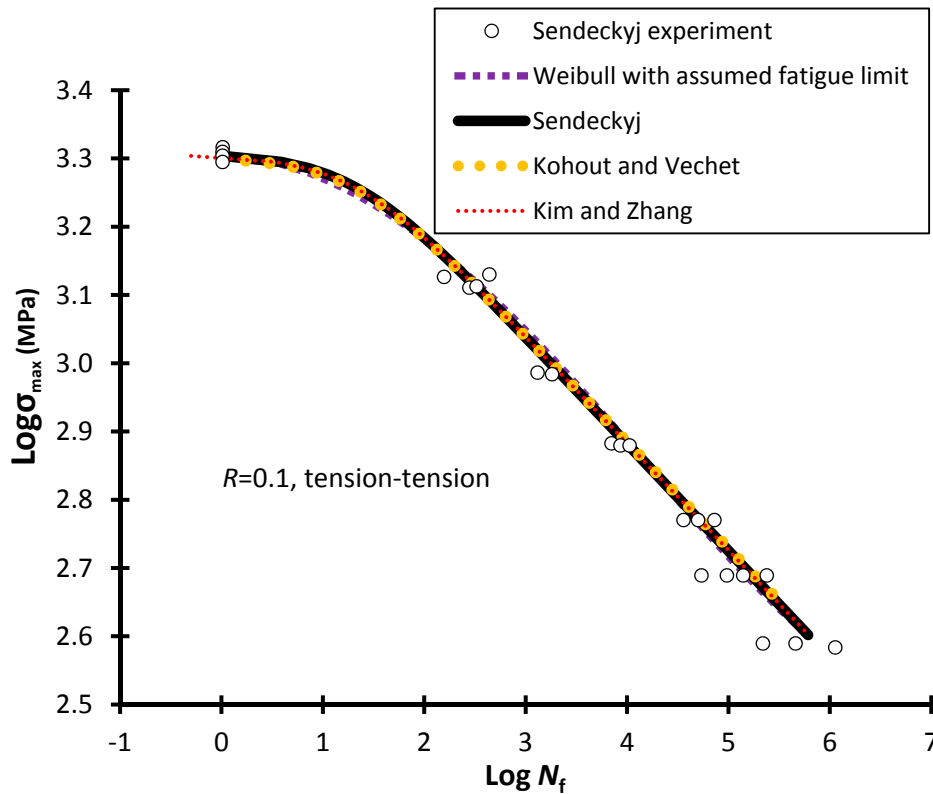


Figure 6. Sendeckyj experimental data at $R = 0.1$ [19] for T-T loading with S-N curves obtained from: Weibull model with $\alpha = 0.088$ and $\beta = 1.9$ for assumed $\sigma_\infty = 250$ MPa; Sendeckyj model with $\alpha = 0.0485$ and $\beta = 0.157$; Kohout and Vechet model with $\alpha = 19.953$ and $\beta = -0.155$; and Kim and Zhang model with $\alpha = 3.13 \times 10^{-27}$, $\beta = 7.381$ for $N_0 = 0.5$.

Figure 7 shows fatigue data obtained from Kawai and Itoh [22] for carbon fiber reinforced epoxy laminates with $\sigma_{uC} = 807$ MPa and $\sigma_{uT} = 1887$ MPa for T-C loading at $R = -0.43$. For comparison purposes of the models, the original experimental data point for $N_f = 0.5$ at σ_{uC} was changed to $N_f = 1$ because of the sensitivity of the S-N curve models to the experimental data point for the initial N_f at σ_{uC} also because Sendeckyj and Weibull models are designed to take $N_f = 1$ at σ_{uC} although Kohout and Vechet model Equation (19) is to take $N_f = 0$ at σ_{uC} while Kim and Zhang model is capable of taking $N_f = 1$ cycle at σ_{uC} as well, (Note $N_f = 0$ is not possible on logarithmic coordinate as discussed earlier.) Accordingly, N_0 in Kim and Zhang model Equations (22) and (23) was set to be 1. As a result, the model fitting parameters were found to be $\alpha = 2.5 \times 10^{-1}$ and $\beta = 0.83$ for Weibull model Equation (8) with an assumed $\sigma_\infty = 0$, $\alpha = 4.485$ and $\beta = 0.078$ for Sendeckyj model Equations (11) and (12), $\alpha = 0.35$ and $\beta = -0.08$ for Kohout and Vechet model Equation (19), and $\alpha = 2.884 \times 10^{-160}$ and $\beta = 54.388$ for Kim and Zhang model Equation Equations (22) and (23). The fitting capabilities of the three models (i.e., Weibull, Sendeckyj, and Kim and Zhang) appear equally good and practically identical. However, as discussed earlier, Kohout and Vechet model Equation (19) is found to be not capable of satisfying the boundary condition at σ_{uC} not because of the experimental data point adjusted to be $N_f = 1$ at σ_{uC} but because of the predetermined S-N curve shape as seen near the first cycle (at $\log N_f = \log \alpha = \log 0.35 = -0.4559$ for the bend) although the degree of deviation from other models is not significant in this case. If the fatigue data point more rapidly decreases at low cycles, the Kohout and Vechet S-N

curve would have more tendency of deviating from the data for the same reason. Also, the points of intersection of the tangent with the two asymptotes at $\log N_f = \log \alpha$ for the bend of S-N curve is arbitrary to some extent.

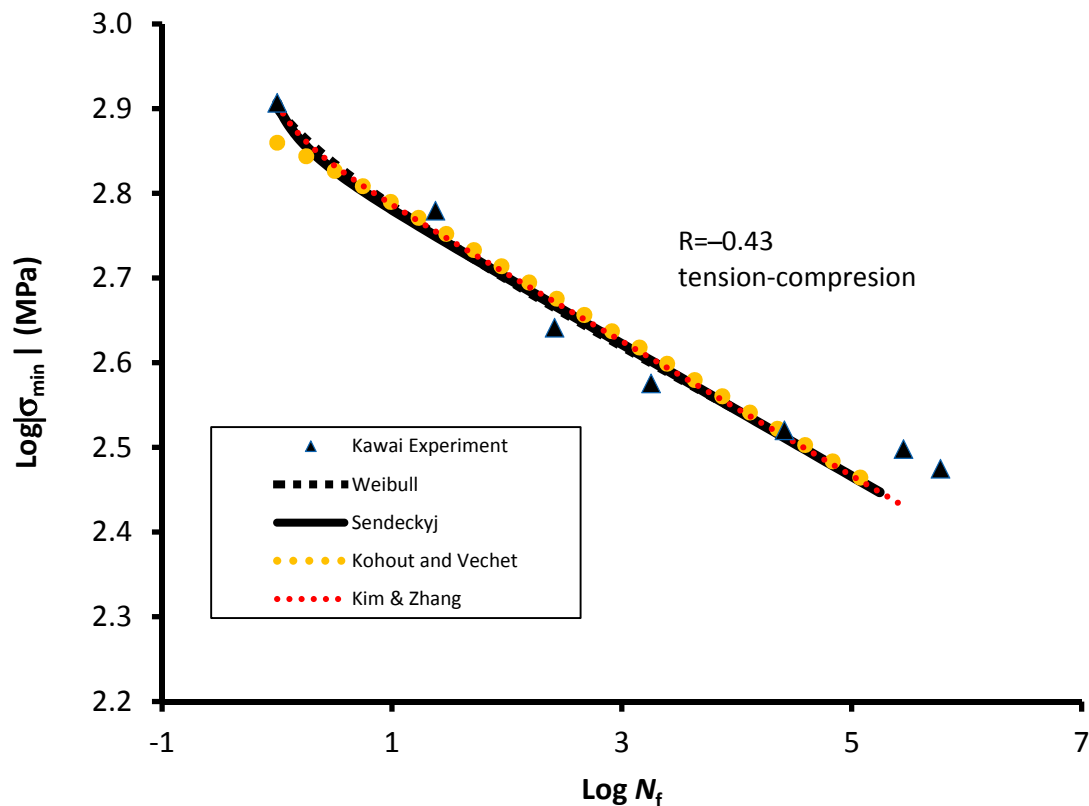


Figure 7. Kawai and Itoh experiment [22] with $\sigma_{uC} = 807$ MPa and $\sigma_{uT} = 1887$ MPa with S-N curves obtained from: Weibull model with $\alpha = 2.5 \times 10^{-1}$ and $\beta = 0.83$, and assumed $\sigma_{\infty} = 0$; Sendeckyj model with $\alpha = 4.485$ and $\beta = 0.078$; Kohout and Vechet model with $\alpha = 0.35$ and $\beta = -0.08$; and Kim and Zhang model with $\alpha = 2.884 \times 10^{-160}$, $\beta = 54.388$ and $N_0 = 1$.

For C-T loading at $R = -3$, Figure 8 shows fatigue experimental data obtained from Kawai and Itoh [22] for carbon fiber reinforced epoxy laminates with $\sigma_{uC} = 807$ MPa and $\sigma_{uT} = 1887$ MPa in comparison with plots from the various S-N curve models. The S-N line shape tendency is similar to those in Figures 5 and 6 such that the fitting capabilities of all the models are again equally good without much sensitivity for the initial N_f at σ_{uC} . In the case of Kohout and Vechet model Equation (19), when α is high for the bend of S-N curve, the sensitivity to the initial experimental point N_f at σ_{uC} decreases as the σ_{min} substantially approaches the σ_{uC} . The model fitting parameters without adjusting the initial experimental point $N_f = 0.5$ at σ_{uC} were found to be $\alpha = 3.5 \times 10^{-3}$ and $\beta = 3.59$ for Weibull model Equation (7) with an assumed $\sigma_{\infty} = 150$ MPa, $\alpha = 0.001985$ and $\beta = 0.08$ for Sendeckyj model Equations (11) and (12), $\alpha = 398$ and $\beta = -0.0775$ for Kohout and Vechet model Equation (19), and $\alpha = 4.295 \times 10^{-38}$ and $\beta = 13.506$ with $N_0 = 0.5$ for Kim and Zhang model.

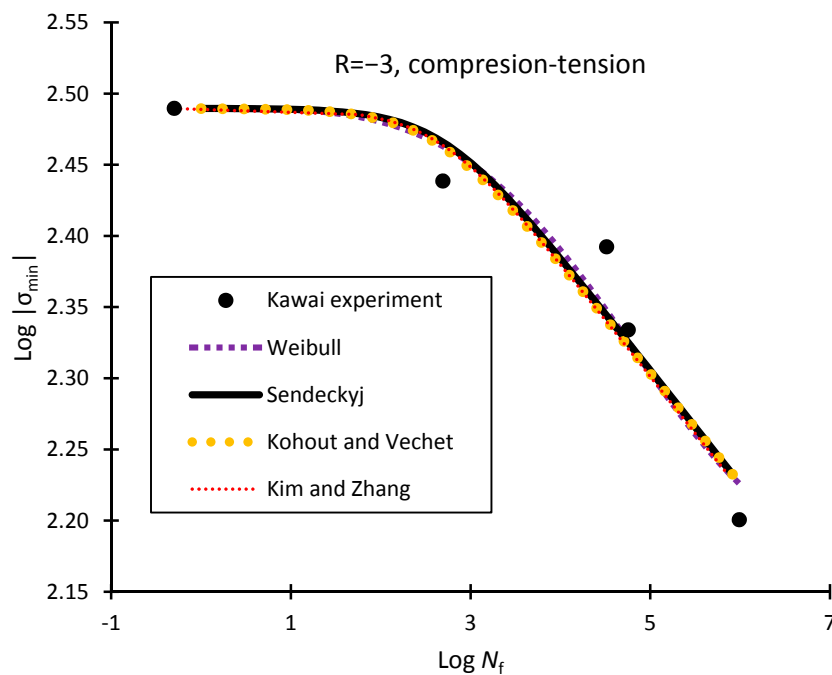


Figure 8. Kawai and Itoh experimental data [22] for carbon fiber reinforced epoxy laminates with $\sigma_{uC} = 807$ MPa and $\sigma_{uT} = 1887$ MPa, and S-N curves obtained from: Weibull model with $\alpha = 3.5 \times 10^{-3}$, $\beta = 3.59$, and assumed $\sigma_{\infty} = 150$ MPa; Sendeckyj model with $\alpha = 0.001985$ and $\beta = 0.08$; Kohout and Vechet model with $\alpha = 398.1$ and $\beta = -0.0775$; and Kim and Zhang model with $\alpha = 4.295 \times 10^{-38}$, $\beta = 13.506$, and $N_0 = 0.5$.

For C-C loading at $R = 10$, an experimental data set obtained from Kawai and Itoh [22] for carbon fiber reinforced epoxy laminates with $\sigma_{uC} = 807$ MPa, ($\sigma_{uT} = 1887$ MPa) is shown in Figure 9. For comparison purposes of the models, an experimental data point is adjusted again to be $N_f = 1$ at σ_{uC} for the same reason in the case of $R = -0.43$ shown in Figure 7 for Weibull, and Sendeckyj models except Kohout and Vechet model Equation (19). Also, N_0 in Kim and Zhang model Equations (22) and (23) was set to be 1. The model fitting parameters were found to be $\alpha = 0.138$ and $\beta = 0.66$ for Weibull model Equation (7) with an assumed $\sigma_{\infty} = 185$ MPa, $\alpha = 1.3$ and $\beta = 0.019$ for Sendeckyj model Equations (11) and (12), $\alpha = 1$ and $\beta = -0.02$ for Kohout and Vechet model Equation (19), and $\alpha = 2.88 \times 10^{-160}$ and $\beta = 54.388$ for Kim and Zhang model with $N_0 = 1$. The fitting capabilities of all the models appear to be equally good and practically identical indicating that all the models can fit the approximate straight line. However, the inherent nature of Kohout and Vechet model from the predetermined S-N curve is again detectable due to the pre-determined points of intersection of the tangent with the two asymptotes at $\log N_f = \log \alpha = \log 1 = 0$ for the bend of S-N curve of the model.

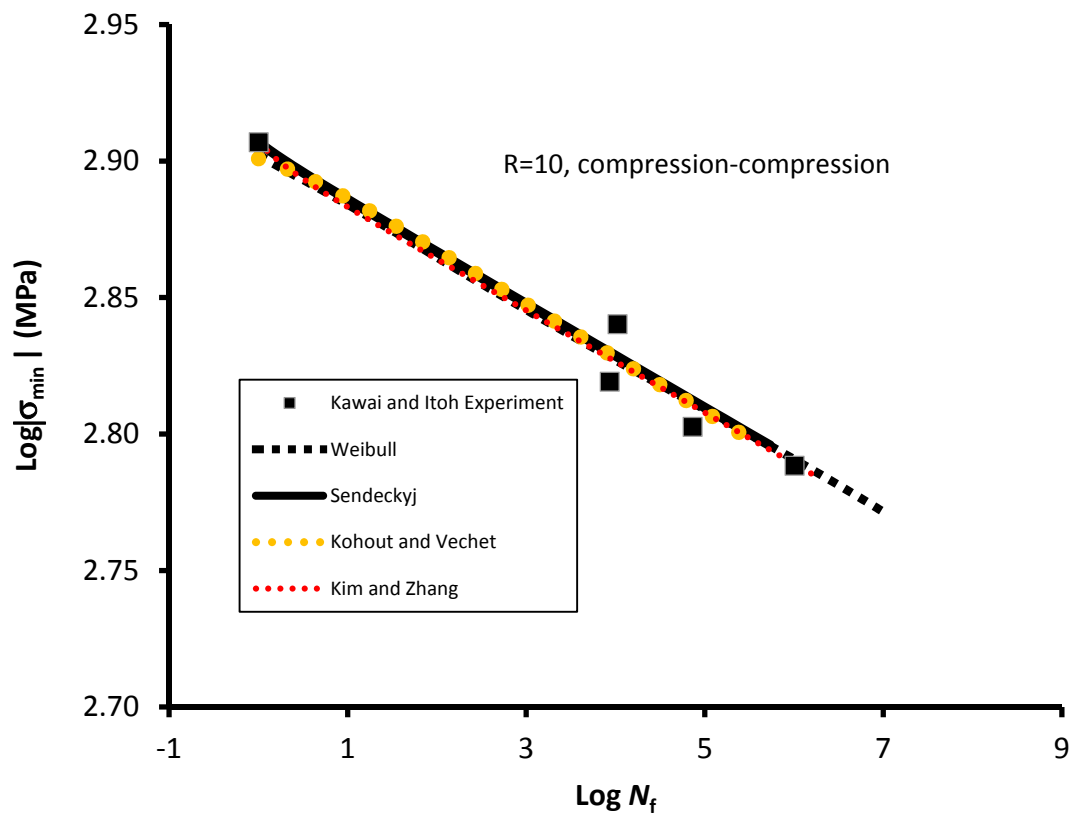


Figure 9. Kawai and Itoh experimental data [22] for carbon fiber reinforced epoxy laminates with $\sigma_{uC} = 807$ MPa and $\sigma_{uT} = 1887$ MPa, and S-N curves obtained from: Weibull model with $\alpha = 0.138$, $\beta = 0.66$, and assumed $\sigma_{\infty} = 185$ MPa; Sendekyj model with $\alpha = 1.3$ and $\beta = 0.019$; Kohout and Vechet model with $\alpha = 1$ and $\beta = -0.02$; and Kim and Zhang model with $\alpha = 2.88 \times 10^{-160}$, $\beta = 54.388$ and $N_0 = 1$.

Table 1 lists selected S-N curve models with two or less fitting parameters for data presentation. The performances of major S-N curve models among those may be summarized as follows: (a) the three models proposed by Weibull, Sendekyj, and Kim and Zhang have the highest fitting capabilities; (b) Kohout and Vechet model has a limited capability of S-N curve line shaping at some stress ratios although its capability, otherwise, is approximately equal to the three models; (b) Sendekyj, and Kim and Zhang models have an advantage over Weibull model for fitting efficiency given that Weibull model needs an additional assumed fatigue limit for curve fitting; and (c) the Kim and Zhang model has an advantage over Sendekyj model for representability of fatigue damage in which the fitting parameters serve as the damage parameters as well. Table 2 lists the four models with parameter values for different stress ratios.

Table 3 lists citation statistics available in the Google Scholar. A citation rate per year for Basquin model is given 12, Kohout and Vechet 4.3, Sendekyj 3.0, Kim and Zhang 0.88, and Weibull 0.21. It brings our attention to the fact that the most incapable model has been the most frequently cited, indicating that many researchers might have compromised the fitting capability for simplicity if they had been aware of capabilities of the existing S-N curve models.

Table 2. Summary of S-N curve models for data characterization proposed by Weibull, Sendeckyj, Kohout and Vechet, and Kim and Zhang.

Experimental Data	Loading	S-N Curve Models	Fitting Parameters			
			α	β	σ_∞ (MPa)	N_0
Weibull (1952) [18] with $\sigma_{uT} = 829$ MPa	$R = -1$ for T-C or C-T loading	Weibull (1952) $\sigma_{\max} = (\sigma_{uT} - \sigma_\infty) \exp[-\alpha(\log N_f)^\beta] + \sigma_\infty$	2.1×10^{-5}	3.8	353	-
			0.003	3.1	0	-
		Sendeckyj (1981) $\sigma_{\max} = \sigma_{uT} / (1 - \alpha + \alpha N_f)^\beta$	0.001	0.093	-	-
		Kohout and Vechet (2001) $\sigma_{\max} = \sigma_{uT} [(N_f + \alpha) / \alpha]^\beta$	776.25	-0.090	-	-
		Kim and Zhang (2001) $N_f = \sigma_{uT}^{-\beta} / [\alpha(\beta - 1)] [(\sigma_{\max} / \sigma_{uT})^{1-\beta} - 1] + N_0$	$10^{-38.44}$	11.81	-	0.5
Sendeckyj (1981) [19] $\sigma_{uT} = 2013$ MPa	$R = 0.1$ for T-T loading	Weibull (1952)	0.088	1.9	250	-
		Sendeckyj (1981)	0.0485	0.157	-	-
		Kohout and Vechet (2001)	19.953	-0.155	-	-
		Kim and Zhang (2001)	3.13×10^{-27}	7.381	-	0.5
Kawai and Itoh (2014) [22] with $\sigma_{uC} = 807$ and $\sigma_{uT} = 1887$ MPa	$R = -0.43$ for T-C loading	Weibull	2.5×10^{-1}	0.83	0	1
		Sendeckyj (1981)	4.485	0.078	-	1
		Kohout and Vechet (2001)	0.35	-0.08	-	-
		Kim and Zhang (2001)	2.88×10^{-160}	54.39	-	1
Kawai and Itoh (2014) [22] with $\sigma_{uC} = 807$ MPa and $\sigma_{uT} = 1887$ MPa	$R = -3$ for C-T loading	Weibull (1952)	3.5×10^{-3}	3.59	150	-
		Sendeckyj (1981)	1.985×10^{-3}	0.08	-	-
		Kohout and Vechet (2001)	398.1	-7.75×10^{-2}	-	-
		Kim and Zhang (2001)	4.295×10^{-38}	13.506	-	0.5
Kawai and Itoh (2014) [22] with $\sigma_{uC} = 807$ MPa and $\sigma_{uT} = 1887$ MPa	$R = 10$ for C-C loading	Weibull (1952)	0.138	0.66	185	1
		Sendeckyj (1981)	1.3	0.019	-	1
		Kohout and Vechet (2001)	1	-0.02	-	-
		Kim and Zhang (2001)	2.88×10^{-160}	54.388	-	1

Table 3. Citations of S-N curve models available in the Google Scholar as of 23 May 2018.

S-N Models	Google Scholar Citations	Citation Rates/Year
Basquin (1910)	1311	12
Weibull (1952)	14	0.21
Sendeckyj (1981)	111	3.0
Kohout and Vechet (2001)	73	4.3
Kim and Zhang (2001)	15	0.88

4.2. S-N Curve Models for Predicting Stress Ratio Effect

The same experimental data sets used for evaluation of S-N curve models for fatigue data characterization will be employed in this section for evaluation of S-N curve models developed for predicting the fatigue stress ratio effect. The best fit provided by the three models (Weibull, Sendeckyj, and Kim and Zhang) will be represented by the Kim and Zhang model as the best fit reference for comparisons. It is noted that D’Amore model Equations (32)–(34), and Epaarachchi and Clausen model Equations (35) and (36) adopt the initial condition $N_f = 1$ at $\sigma_{max} = \sigma_{uT}$ while Poursatip and Beaumont model Equations (29) and (30) adopts $N_f = 0$ at σ_{uC} , which does not exist on logarithmic coordinate. Therefore, the same condition i.e., $N_f = 1$ at $\sigma_{max} = \sigma_{uT}$ as those in Figures 7 and 9 was employed for comparison purposes such that the other models and experimental data were accordingly adjusted. Experimental data and plots will be in lin-log coordinates.

An experimental data set from Weibull [18] is shown in Figure 10 in comparison with S-N curves generated from the various models for $R = -1$: Kim and Zhang model Equations (22) and (23) as the reference with $\alpha = 3.63 \times 10^{-39}$ and $\beta = 11.809$ for $N_0 = 1$; Poursatip and Beaumont model Equation (30) with $\alpha = 17,000$ and an added $N_0 = 1$; D’Amore model Equation (34) with $\alpha' = 0.053$ and $\beta = 0.2$; and Epaarachchi and Clausen model Equation (36) with $\alpha' = 0.0007$ and $\beta = 0.245$. It is seen that all the models do not agree with the reference performed by the three models or Kim and Zhang model. The Poursatip and Beaumont model, however, appears closer to the reference fit than the other two models. It was found, at the same time, that the S-N line shape of Poursatip and Beaumont model is controlled by a single fitting parameter α which only allows it to move around the first data point (for $N_f = 1$ at $\sigma_{max} = \sigma_{uT}$) as the hinge without much controlling the shape. On the other hand, the fitting capabilities of D’Amore, and Epaarachchi and Clausen models appear relatively poor, given that radii of the curvature of the S-N curves at low cycles are too large compared to the reference fit. A possible reason for this is that the derivation may not be validly conducted as discussed earlier. Also, it would not be surprising to find that D’Amore, and Epaarachchi and Clausen models are practically identical in this case probably due to their similarities in expression and derivation [see Equations (34) and (36)]. The only difference made by the exponent 1.6 in the Epaarachchi and Clausen model Equation (36) is found to be reflected only in values of fitting parameters α' and β .

An experimental data set from Sendeckyj [19] obtained for glass reinforced epoxy laminates with $\sigma_{uT} = 2013$ MPa is shown in Figure 11 in comparison with S-N curves generated from the various models for $R = 0.1$ under T-T loading. The fitting parameters were found as follows: $\alpha = 10^{-26.505}$ and $\beta = 7.3813$ for Kim and Zhang model Equations (22) and (23) with $N_0 = 1$; $\alpha = 60$ and an added $N_0 = 1$ for Poursatip and Beaumont model Equation (30); $\alpha' = 0.033$ and $\beta = 0.44$ for D’Amore model Equation (34); $\alpha' = 0.00035$ and $\beta = 0.51$ for Epaarachchi and Clausen model Equation (36). D’Amore, and Epaarachchi and Clausen models appear improved for fitting capabilities compared to those for $R = -1$ (Figure 10) probably because of the rapid decrease in experimental data at low cycles as expected from their S-N curve performances shown in Figure 10 although clear deviations from the best fit are noticed. However, the added exponent 1.6 in Equation (36) does not seem to greatly improve the D’Amore model Equation (34). A fitting capability of Poursatip and Beaumont model appear still good although a slight difference from the best fit is noticed.

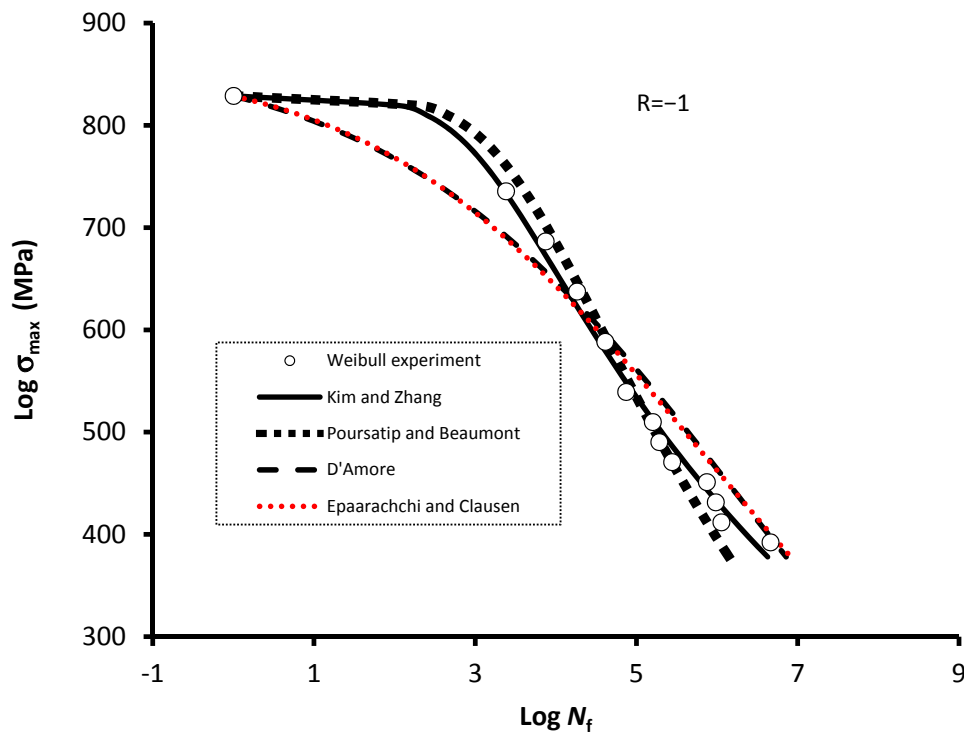


Figure 10. Weibull experimental data at $R = -1$ [18] plotted with data points having a probability of 50% failure for Bofors FR 76 Steel rotating beam test with $\sigma_{uT} = 829$ MPa, and S-N curves obtained from: Kim and Zhang model with $\alpha = 3.63 \times 10^{-39}$, $\beta = 11.809$, and $N_0 = 1$; Poursatip and Beaumont model with $\alpha = 17,000$ and added $N_0 = 1$; D'Amore model with $\alpha' = 0.053$ and $\beta = 0.2$; and Epaarachchi and Clausen model with $\alpha' = 0.0007$ and $\beta = 0.245$.

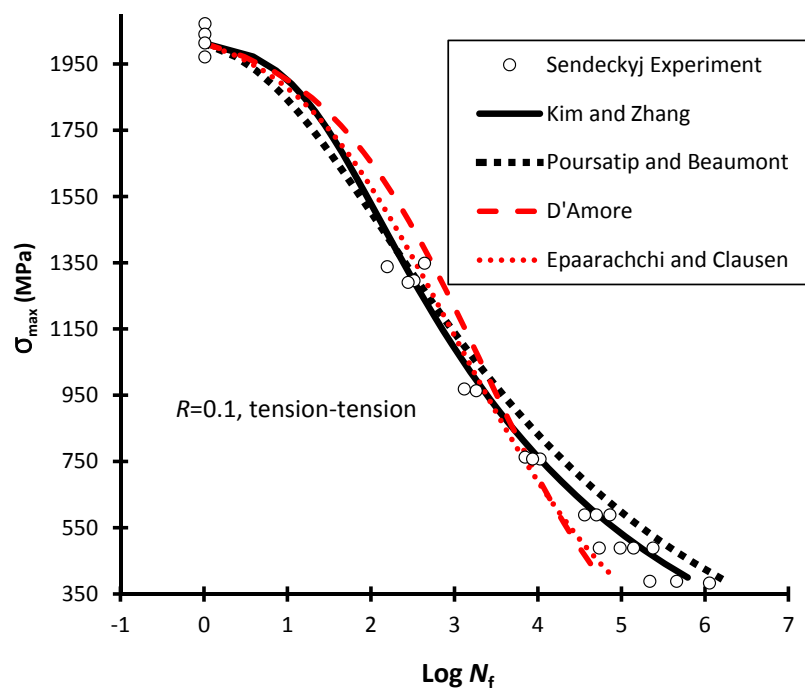


Figure 11. Sendeckyj experimental data at $R = 0.1$ for glass reinforced epoxy laminates with $\sigma_{uT} = 2013$ MPa [19] under T-T loading, and S-N curves obtained from: Kim and Zhang model with $\alpha = 10^{-26.505}$, $\beta = 7.3813$, and $N_0 = 1$; Poursatip and Beaumont model with $\alpha = 60$ and added $N_0 = 1$; D'Amore with $\alpha' = 0.033$ and $\beta = 0.44$; and Epaarachchi and Clausen model with $\alpha' = 0.00035$ and $\beta = 0.51$.

Figure 12 shows experimental data from Kawai and Itoh [22] with $\sigma_{uC} = 807$ MPa and ($\sigma_{uT} = 1887$ MPa) for $R = -0.43$ in comparison with various models: Kim and Zhang model Equations (22) and (23) with $\alpha = 8.18 \times 10^{-41}$ and $\beta = 13.6$ for $N_0 = 1$; Poursatip and Beaumont model Equation (30) with $\alpha = 29$ and added $N_0 = 1$; D'Amore model Equation (34) with $\alpha' = 0.3$ and $\beta = 0.19$; and Epaarachchi and Clausen model Equation (36) with $\alpha' = 0.0169$ and $\beta = 0.14$. The Epaarachchi and Clausen model appear very close to the reference fit (or Kim and Zhang model) while Poursatip and Beaumont, and D'Amore models noticeably deviated from the reference fit. The difference in behavior between D'Amore model, and Epaarachchi and Clausen model indicates that the added exponent 1.6 in Equation (36) noticeably affects the S-N curve shape in this case.

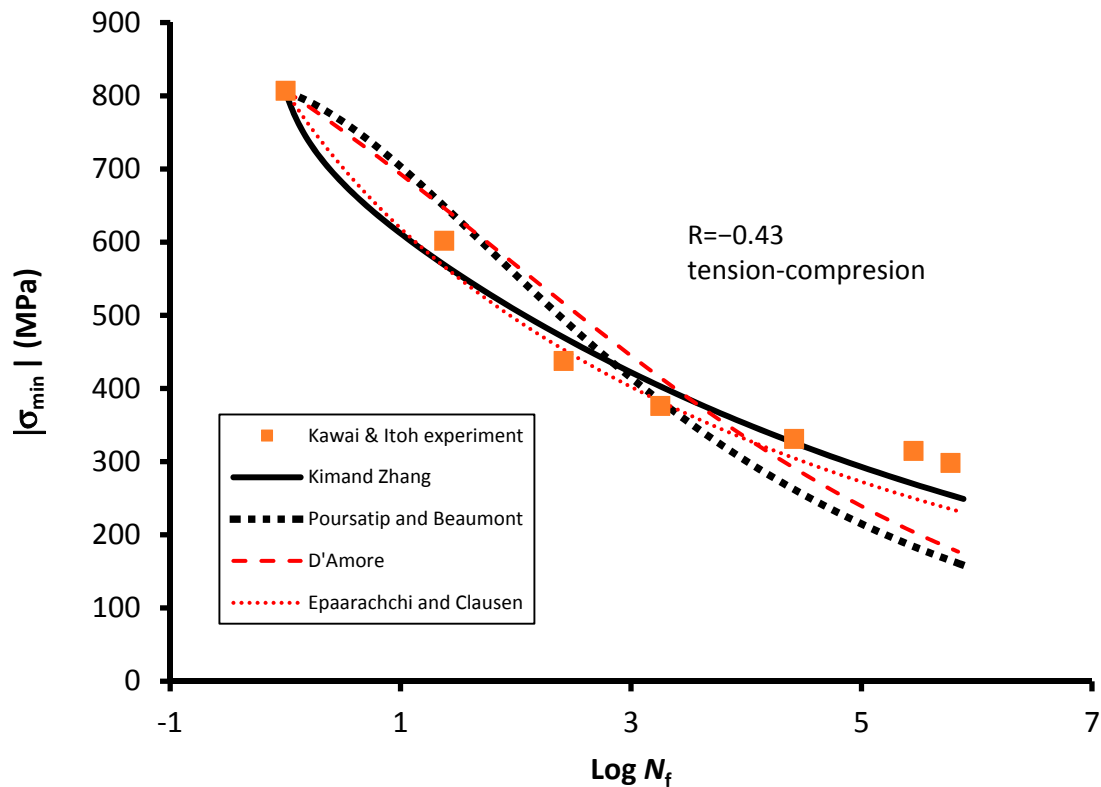


Figure 12. Kawai and Itoh experiment at $R = -0.43$ [22] with $\sigma_{uC} = 807$ MPa and $\sigma_{uT} = 1887$ MPa, and S-N curves obtained from: Kim and Zhang model with $\alpha = 8.18 \times 10^{-41}$, $\beta = 13.6$, and $N_0 = 1$; Poursatip and Beaumont model $\alpha = 29$ and added $N_0 = 1$; D'Amore model with $\alpha' = 0.3$ and $\beta = 0.19$; and Epaarachchi and Clausen model with $\alpha' = 0.0169$ and $\beta = 0.14$. An experimental data point for $N_f = 0.5$ cycle was adjusted to have the initial condition $N_f = 1$ at σ_{uC} for comparison purposes.

An experimental data set from Kawai and Itoh [22] with $\sigma_{uC} = 807$ MPa, ($\sigma_{uT} = 1887$ MPa) for $R = -3$ representing C-T loading is shown in Figure 13 with S-N curves generated from the various models: Kim and Zhang model with $\alpha = 4.3 \times 10^{-38}$, $\beta = 13.506$, and $N_0 = 1$; Poursatip and Beaumont model Equation (30) with $\alpha = 11,000$ and added $N_0 = 1$; for D'Amore model Equation (34) with $\alpha' = 0.053$ and $\beta = 0.2$; for the Epaarachchi and Clausen model Equation (36) with $\alpha' = 0.001$ and $\beta = 0.25$. The fitting capabilities of all models appear to be good but differences between models are not as obvious as those for $R = -1$ in Figure 10 because the experimental data set is relatively small compared to that for $R = -1$. However, the same tendencies of D'Amore, and Epaarachchi and Clausen models are seen such that the radii of the curvature of S-N curve at low cycles is still large. Also, it is noted that D'Amore, and Epaarachchi and Clausen models behave similarly again without much effect of the modified exponent 1.6 in Equation (36) on the S-N curve shape.

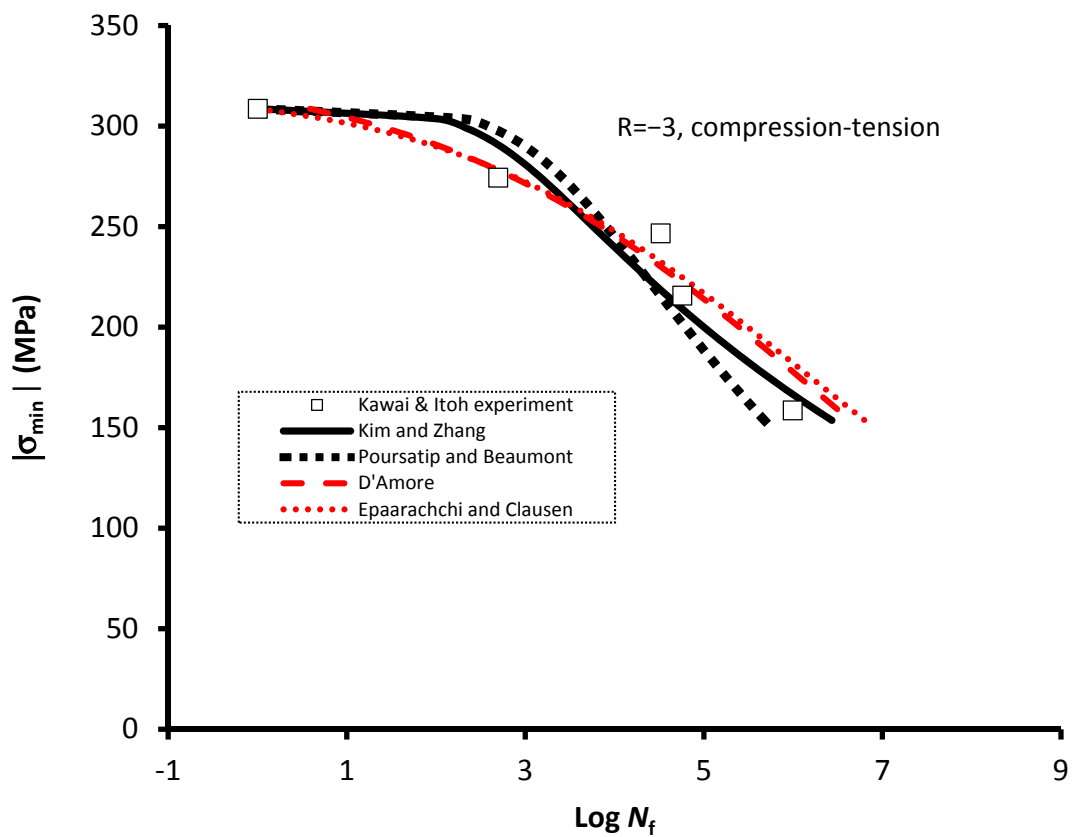


Figure 13. Kawai and Itoh experimental data at $R = -3$ [22] for carbon fiber reinforced epoxy laminates with $\sigma_{UC} = 807$ MPa and $\sigma_{uT} = 1887$ MPa, and S-N curves obtained from: Kim and Zhang model with $\alpha = 4.3 \times 10^{-38}$, $\beta = 13.506$, and $N_0 = 1$; Poursatip and Beaumont model with $\alpha = 11,000$ and added $N_0 = 1$; D'Amore model with $\alpha' = 0.053$ and $\beta = 0.2$; and Epaarachchi and Clausen model with $\alpha' = 0.001$ and $\beta = 0.25$.

Figure 14 shows an experimental data set from Kawai and Itoh [22] with $\sigma_{uC} = 807$ MPa ($\sigma_{uT} = 1887$ MPa) for $R = 10$ with S-N curves generated from the various models: the Kim and Zhang model Equations (22) and (23) with $\alpha = 2.9 \times 10^{-160}$ and $\beta = 54.388$ for $N_0 = 1$; the Poursatip and Beaumont model Equation (30) with $\alpha = 719$ and added $N_0 = 1$; the D'Amore model, Equation (34), with $\alpha' = 0.043$ and $\beta = 0.01$; the Epaarachchi and Clausen model Equation (36) with $\alpha' = 0.0075$ and $\beta = 0.048$. The fitting capabilities of the D'Amore, and Epaarachchi and Clausen models appear to be practically identical to the reference fit (or Kim and Zhang model). In contrast, the Poursatip and Beaumont model significantly deviates from the reference fit and seems to have a strong tendency of producing the concave-down S-N curve at low cycles. Judging from the earlier observations, the Poursatip and Beaumont model seems incapable of producing other shapes than the concave-down S-N curve at low cycles regardless of stress ratio. A possible reason for this may be due to some defects during derivation as discussed earlier even though Equation (27) satisfies Equation (1).

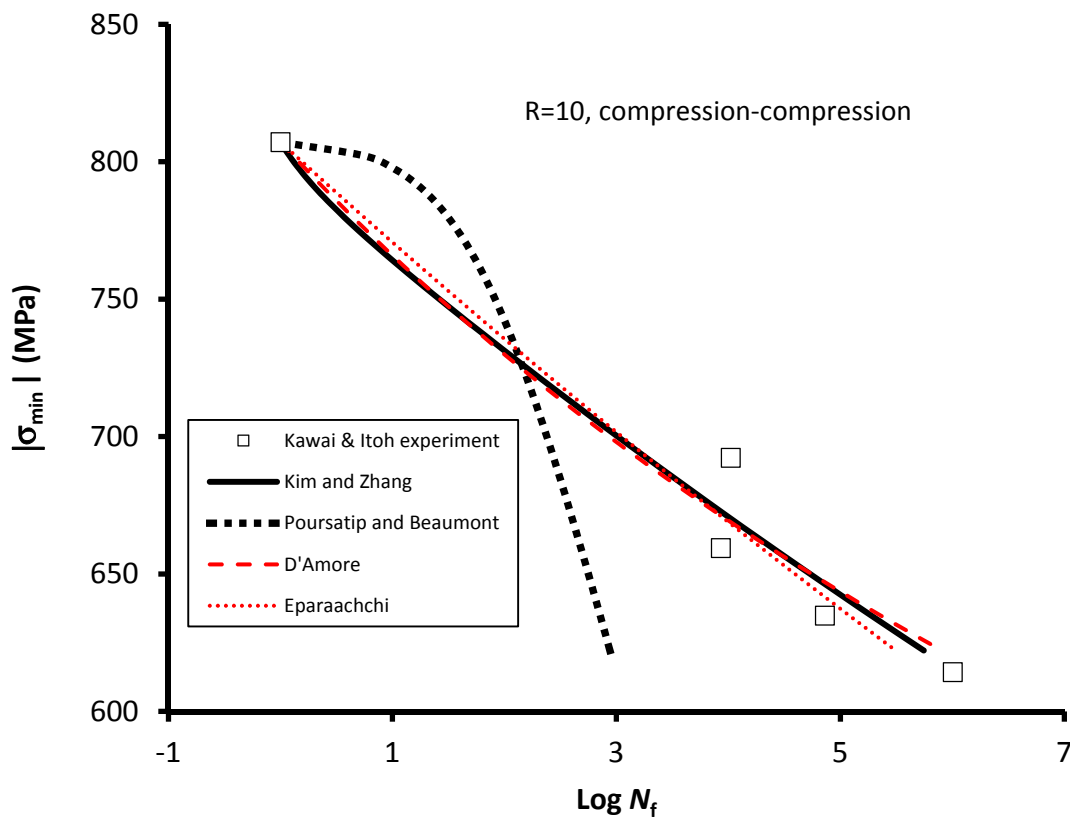


Figure 14. Kawai and Itoh experimental data at $R = 10$ [22] for carbon fiber reinforced epoxy laminates with $\sigma_{uC} = 807$ MPa and $\sigma_{uT} = 1887$ MPa, and S-N curves obtained from: Kim and Zhang model with $\alpha = 2.9 \times 10^{-160}$, $\beta = 54.388$, and $N_0 = 1$; Poursatip with $\alpha = 719$ and added $N_0 = 1$; D'Amore model with $\alpha' = 0.043$ and $\beta = 0.01$; and Epaarachchi and Clausen model with $\alpha' = 0.0075$ and $\beta = 0.048$.

In summary, the three S-N curve models developed for predicting for stress ratio effect appear inferior to those best performed for data characterization. They are listed in Table 4 and their performances are summarized.

5. Conclusions

S-N curve models proposed by Weibull, Sendekyj, and Kim and Zhang for fatigue data characterization have been found to have the highest fitting capabilities for experimental fatigue data obtained by Weibull for $R = -1$, Sendekyj for $R = 0.1$, and Kawai and Itoh for $R = -0.43, -3$, and 10 . The Kohout and Vechet model was also found to have good fitting capabilities but with a limitation for shaping S-N curve at some stress ratios (e.g., $R = -0.43$). Also, S-N curve models developed for predicting the effect of stress ratio were found to be relatively inferior in fitting capability to those developed directly for data characterization. The Kim and Zhang model appeared to have an advantage over the Weibull and Sendekyj models for representing the fatigue damage at failure, which may be further useful for developing applicative models.

Table 4. S-N curve models developed for stress ratio effect.

S-N Curve Models	Capability of Curve Fitting and Applicability to Different Stress Ratios		Number of Fitting Parameters	Relation with Physical Properties		
	R	Capability		Boundary at Initial N_f	Damage Representation	Satisfaction of $\frac{\partial D_{fT}}{\partial \sigma_{max}} = -A$
Poursartip and Beaumont (1986) $N_f = \alpha \left(\frac{\sigma_{max}}{\sigma_{uT}} \right)^{-6.393} \left(\frac{\sigma_{uT} - \sigma_{max}}{\sigma_{uT}} \right)$	1 0.1 -0.43 -3 10	Good Good Poor Reasonable Poor	1	Yes	Partially Yes	Yes
D'Amore et al. (1996) $N_f = \left[\frac{\sigma_{uT} - \sigma_{max}}{\alpha' \sigma_{max}} + 1 \right]^{1/\beta}$	-1 0.1 -0.43 -3 10	Poor Reasonable Poor Reasonable Good	2	Yes	N/A	N/A
Epaarachchi and Clausen (2003) $N_f = \left(\frac{\sigma_{uT} - \sigma_{max}}{\alpha' (\sigma_{max})^{1.6}} + 1 \right)^{1/\beta}$	-1 0.1 -0.43 -3 10	Poor Reasonable Good Reasonable Good	2	Yes	N/A	N/A

Funding: This research received no external funding.

Acknowledgments: One of authors (Burhan) gratefully acknowledges the scholarship provided by the Ministry of Higher Education of Malaysia.

Conflicts of Interest: The authors declare no conflict of interest.

References

1. Broek, D. *Elementary Engineering Fracture Mechanics*; Sijthoff & Noordhoff: Amsterdam, The Netherlands, 1978; ISBN 90-286-0208-9.
2. Kitagawa, H.; Takashima, S. Application of fracture mechanics to very small fatigue cracks or the cracks in the early stage. In Proceedings of the Second International Conference on Mechanical Behavior of Materials, American Society for Metals, Materials Park, Boston, MA, USA, 16–20 August 1976; pp. 627–631.
3. Weibull, W. A Statistical Distribution Function of wide Applicability. *J Appl. Mech.* **1951**, *18*, 293–297.
4. Wang, S.S.; Chim, E.S.-M. Fatigue Damage and Degradation in Random Short-Fiber SMC Composite. *J. Compos. Mater.* **1983**, *17*, 114–134. [[CrossRef](#)]
5. Kawai, M.; Hachinohe, A. Two-stress level fatigue of unidirectional fiber–metal hybrid composite: GLARE 2. *Int. J. Fatigue* **2002**, *24*, 567–580. [[CrossRef](#)]
6. Kawai, M.; Saito, S. Off-axis strength differential effects in unidirectional carbon/epoxy laminates at different strain rates and predictions of associated failure envelopes. *Compos. Part A* **2009**, *40*, 1632–1649. [[CrossRef](#)]
7. Rhines, F.N. Quantitative microscopy and fatigue mechanisms. In *Fatigue Mechanisms, Proceedings of the ASTM-NBS-NSF Symposium, Kansas City, MO, USA, 21–22 May 1978*; ASTM STP 675; Fong, J.T., Ed.; American Society for Testing and Materials: Philadelphia, PA, USA, 1979; pp. 23–46.
8. Rupean, J.; Bhowal, P.; Eylon, D.; McEvily, A.J. On the process of subsurface fatigue crack initiation in Ti-6Al-4V. In *Fatigue Mechanisms, Proceedings of the ASTM-NBS-NSF Symposium, Kansas City, MO, USA, 21–22 May 1978*; ASTM STP 675; Fong, J.T., Ed.; American Society for Testing and Materials: Philadelphia, PA, USA, 1979; pp. 47–68.
9. Karadag, M.; Stephens, R.I. The influence of high R ratio on unnotched fatigue behavior of 1045 steel with three different heat treatments. *Int. J. Fatigue* **2003**, *25*, 191–200. [[CrossRef](#)]
10. Schütz, W. A history of fatigue. *Eng. Fract. Mech.* **1996**, *54*, 263–300. [[CrossRef](#)]
11. Braithwaite, F. On the fatigue and consequent fracture of metals. In *Minutes of the Proceedings of Civil Engineers*; Institution of Civil Engineers: London, UK, 1854; Volume 13, pp. 463–467.
12. Wöhler, A. *Ueber die Festigkeits-Versuche mit Eisen und Stahl*; Ernst & Korn: Berlin, German, 1870; pp. 74–106.
13. Gerber, W.Z. Bestimmung der zulässigen Spannungen in Eisen-Constructionen. [Calculation of the allowable stresses in iron structures]. *Z Bayer Arch. Ing. Ver.* **1874**, *6*, 101–110.
14. Weyrauch, P.J.J. *Strength and Determination of the Dimensions of Structures of Iron and Steel with Reference to the Latest Investigations*, 3rd ed.; Du Bois, A.J., Translator; John Wiley and Sons: New York, NY, USA, 1891.
15. Goodman, J. *Mechanics Applied to Engineering*, 1st ed.; Longmans, Green and Co.: London, UK, 1899.
16. Soderberg, C.R. Factor of safety and working stress. *Trans. Am. Soc. Test Matls.* **1930**, *52*, 13–28.
17. Basquin, O.H. The exponential law of endurance test. *ASTM STP* **1910**, *10*, 625–630.
18. Weibull, W. The statistical aspect of fatigue failures and its consequences. In *Fatigue and Fracture of Metals*; Massachusetts Institute of Technology; John Wiley & Sons: New York, NY, USA, 1952; pp. 182–196.
19. Sendeckyj, G.P. Fitting models to composite materials fatigue data. In *Test Methods and Design Allowables for Fibrous Composites*; ASTM STP 734; Chamis, C.C., Ed.; ASTM International: West Conshohocken, PA, USA, 1981; pp. 245–260.
20. Hwang, W.; Han, K.S. Cumulative damage models and multi-stress fatigue life prediction. *J. Compos. Mater.* **1986**, *20*, 125–153. [[CrossRef](#)]
21. Kawai, M.; Koizumi, M. Nonlinear constant fatigue life diagrams for carbon/epoxy laminates at room temperature. *Compos. Part A Appl. Sci. Manuf.* **2007**, *38*, 2342–2353. [[CrossRef](#)]
22. Kawai, M.; Itoh, N. A failure-mode based anisomorphic constant life diagram for a unidirectional carbon/epoxy laminate under off-axis fatigue loading at room temperature. *J. Compos. Mater.* **2014**, *48*, 571–592. [[CrossRef](#)]
23. Palmgren, A. Die Lebensdauer von Kugellagern. *Schwed Warmewirtschaft* **1924**, *68*, 339–341.

24. Hwang, W.; Han, K.S. Fatigue of Composites—Fatigue Modulus Concept and Life Prediction. *J. Compos. Mater.* **1986**, *20*, 154–165. [[CrossRef](#)]
25. Poursartip, A.; Ashby, M.F.; Beaumont, P.W.R. The fatigue damage mechanics of carbon fibre composite laminate: I—Development of the model. *Compos. Sci. Technol.* **1986**, *25*, 193–218. [[CrossRef](#)]
26. Poursartip, A.; Beaumont, P.W.R. The fatigue damage mechanics of carbon fibre composite laminate: II—Life prediction. *Compos. Sci. Technol.* **1986**, *25*, 283–299. [[CrossRef](#)]
27. Eskandari, H.; Kim, H.S. A Theory for mathematical framework and fatigue damage function for the S-N plane. In *Fatigue and Fracture Test Planning, Test Data Acquisitions, and Analysis*; ASTM STP1598; Wei, Z., Nikbin, K., McKeighan, P.C., Harlow, D.G., Eds.; ASTM International: West Conshohocken, PA, USA, 2017; pp. 299–336.
28. Mao, W.; Ringsberg, J.W.; Rychlik, I.; Li, Z. Theoretical development and validation of a fatigue model for ship routing. *Ships Offshore Struct.* **2012**, *7*, 399–415. [[CrossRef](#)]
29. Miner, M.A. Cumulative damage in fatigue. *Am. Soc. Mech. Eng. J. Appl. Mech.* **1945**, *12*, 159–164.
30. Philippidis, T.P.; Passipoularidis, V.A. Residual strength after fatigue in composites: Theory vs. experiment. *Int. J. Fatigue* **2007**, *29*, 2104–2116. [[CrossRef](#)]
31. Post, N.; Case, S.; Lesko, J. Modeling the variable amplitude fatigue of composite materials: A review and evaluation of the state of the art for spectrum loading. *Int. J. Fatigue* **2008**, *30*, 2064–2086. [[CrossRef](#)]
32. Eskandari, H.; Kim, H.S. A theory for mathematical framework of fatigue damage on S-N plane. *Key Eng. Mater.* **2015**, *627*, 117–120. [[CrossRef](#)]
33. Rege, K.; Pavlou, D.G. A one-parameter nonlinear fatigue damage accumulation model. *Int. J. Fatigue* **2017**, *98*, 234–246. [[CrossRef](#)]
34. Weibull, W. Chapter VIII, Presentation of Results. In *Fatigue Testing and Analysis of Results*; Pergamon Press: Oxford, UK; London, UK; New York, NY, USA; Paris, France, 1961.
35. Kohout, J.; Vechet, S. A new function for fatigue curves characterization and its multiple merits. *Int. J. Fatigue* **2001**, *23*, 175–183. [[CrossRef](#)]
36. Nijssen, R.P.L. Phenomenological fatigue analysis and life modelling. In *Fatigue Life Prediction of Composites and Composite Structures*; Vassilopoulos, A.P., Ed.; Woodhead publishing Limited: Oxford, UK; Cambridge, UK; New Delhi, India, 2010; pp. 45–78.
37. Xiong, J.J.; Shenoi, R.A. *Fatigue and Fracture Reliability Engineering*; Springer: London, UK; Dordrecht, The Netherlands; Heidelberg, German; New York, NY, USA, 2011.
38. Burhan, I.; Kim, H.S.; Thomas, S. A refined S-N curve model. In Proceedings of the International Conference on Sustainable Energy, Environment and Information (SEEIE 2016), Bangkok, Thailand, 20–21 March 2016; pp. 412–416.
39. Passipoularidis, V.A.; Philippidis, T.P.; Brondsted, P. Fatigue life prediction in composites using progressive damage modelling under block and spectrum loading. *Int. J. Fatigue* **2011**, *33*, 132–144. [[CrossRef](#)]
40. Fatemi, A.; Yang, L. Cumulative fatigue damage and life prediction theories: A survey of the state of the art for homogeneous materials. *Int. J. Fatigue* **1998**, *23*, 9–34. [[CrossRef](#)]
41. Yang, L.; Fatemi, A. Cumulative Fatigue Damage Mechanisms and Quantifying Parameters: A Literature Review. *J. Test. Eval.* **1998**, *26*, 89–100.
42. Bathias, C.; Pineau, A. *Fatigue of Materials and Structures-Application to Design and Damage*; ISTE: London, UK; Wiley: Hoboken, NJ, USA, 2011.
43. Christian, L. Chapter 2, Fatigue Damage. In *Mechanical Vibration and Shock Analysis*, 3rd ed.; John Wiley & Sons: London, UK; Hoboken, NJ, USA, 2014; Volume 4.
44. O'Brian, T.K.; Reifsnider, K.L. Fatigue damage evaluation through stiffness measurements in boron-epoxy laminates. *J. Compos. Mater.* **1981**, *15*, 55–70.
45. Marin, J. *Mechanical Behavior of Engineering Materials*; Prentice-Hall: Englewood Cliffs, NJ, USA, 1962.
46. Subramanyan, S. A cumulative damage rule based on the knee point of the SN curve. *J. Eng. Mater. Technol.* **1976**, *98*, 316–321. [[CrossRef](#)]
47. Mandell, J.F.; Meier, U. Effects of stress ratio, frequency, and loading time on the tensile fatigue of glass-reinforced epoxy. In *Long-Term Behavior of Composites*; ASTM STP 813; O'Brien, T.K., Ed.; American Society for Testing and Materials: Philadelphia, PA, USA, 1983; pp. 55–77.
48. Bond, I.P.; Farrow, I.R. Fatigue life prediction under complex loading for XAS/914 CFRP incorporating a mechanical fastener. *Int. J. Fatigue* **2000**, *22*, 633–644. [[CrossRef](#)]

49. Tamuz, V.; Dzelzitis, K.; Reifsnider, K. Fatigue of Woven Composite Laminates in Off-Axis Loading II. Prediction of the Cyclic Durability. *Appl. Compos. Mater.* **2004**, *11*, 281–292. [[CrossRef](#)]
50. Gathercole, N.; Reiter, H.; Adam, T.; Harris, B. Life prediction for fatigue of T800/5245 carbon-fibre composites: I. Constant-amplitude loading. *Fatigue* **1994**, *16*, 523–532. [[CrossRef](#)]
51. Adam, T.; Gathercole, N.; Reiter, H.; Harris, B. Life prediction for fatigue of T800/5245 carbon-fibre composites: II. Variable amplitude loading. *Fatigue* **1994**, *16*, 533–547. [[CrossRef](#)]
52. Beheshty, M.H.; Harris, B.; Adam, T. An empirical fatigue-life model for high-performance fibre composites with and without impact damage. *Compos. Part A Appl. Sci. Manuf.* **1999**, *30*, 971–987. [[CrossRef](#)]
53. Bathias, C. There is no infinite fatigue life in metallic materials. *Fatigue Fract. Eng. Mater. Struct.* **1999**, *22*, 559–565. [[CrossRef](#)]
54. Stromeyer, C.E. The Determination of Fatigue Limits under Alternating Stress Conditions. *Proc. R. Soc. A Math. Phys. Eng. Sci.* **1914**, *90*, 411–425. [[CrossRef](#)]
55. Henry, D.L. A Theory of Fatigue-Damage Accumulation in Steel. *Trans. ASME* **1955**, 913–918.
56. Ellyin, F. *Cyclic Strain Energy Density as a Criterion for Multiaxial Fatigue Failure, Biaxial and Multiaxial Fatigue, EGF2*; Brown, M.W., Miller, K.J., Eds.; Mechanical Engineering Publications: London, UK, 1989; pp. 571–583.
57. Ellyin, F.; El-Kadi, H. A fatigue failure criterion for fibre reinforced composite laminae. *Compos. Struct.* **1990**, *15*, 61–74. [[CrossRef](#)]
58. Kensche, C.W. Influence of composite fatigue properties on lifetime predictions of sailplanes. In Proceedings of the XXIV OSTIV Congress, Vol XIX, No 3, Omarama, New Zealand, 12–19 January 1995; pp. 69–76.
59. Kulawinski, D.; Kolmorgen, R.; Biermann, H. Application of Modified Stress-Strain Approach for the Fatigue-Life Prediction of a Ferritic, an Austenitic and a Ferritic-Austenitic Duplex Steel under Isothermal and Thermo-Mechanical Fatigue. *Steel Res. Int.* **2016**, *87*, 1095–1104. [[CrossRef](#)]
60. Kim, H.S.; Zhang, J. Fatigue Damage and Life Prediction of Glass/Vinyl Ester Composites. *J. Reinf. Plast. Compos.* **2001**, *20*, 834–848. [[CrossRef](#)]
61. Kassapoglou, C. Fatigue life prediction of composite structures under constant amplitude loading. *J. Compos. Mater.* **2007**, *41*, 2737–2754. [[CrossRef](#)]
62. Kassapoglou, C. Fatigue of composite materials under spectrum loading. *Compos. Part A* **2010**, *41*, 663–669. [[CrossRef](#)]
63. Owen, M.; Howe, R. The accumulation of damage in a glass-reinforced plastic under tensile and fatigue loading. *J. Phys. D Appl. Phys.* **1972**, *5*, 1637–1649. [[CrossRef](#)]
64. Yang, J.N.; Liu, M.D. Residual Strength Degradation Model and Theory of Periodic Proof Tests for Graphite/Epoxy Laminates. *J. Compos. Mater.* **1977**, *11*, 176–203. [[CrossRef](#)]
65. Yang, J.N. Fatigue and Residual Strength Degradation for Graphite/Epoxy Composites Under Tension-Compression Cyclic Loadings. *J. Compos. Mater.* **1978**, *12*, 19–39. [[CrossRef](#)]
66. Rotem, A. Residual Strength after Fatigue Loading. *Int. J. Fatigue* **1988**, *10*, 27–31. [[CrossRef](#)]
67. D'Amore, A.; Caprino, G.; Stupak, P.; Zhou, J.; Nicolais, L. Effect of stress ratio on the flexural fatigue behaviour of continuous strand mat reinforced plastics. *Sci. Eng. Compos. Mater.* **1996**, *5*, 1–8. [[CrossRef](#)]
68. Caprino, G.; Giorlea, G. Fatigue lifetime of glass fabric/epoxy composites. *Compos. Part A Appl. Sci. Manuf.* **1999**, *30*, 299–304. [[CrossRef](#)]
69. Epaarachchi, J.A.; Clausen, P.D. An empirical model for fatigue behavior prediction of glass fibre-reinforced plastic composites for various stress ratios and test frequencies. *Compos. Part A Appl. Sci. Manuf.* **2003**, *34*, 313–326. [[CrossRef](#)]
70. Epaarachchi, J.A. Effects of static-fatigue (tension) on the tension-tension fatigue life of glass fibre reinforced plastic composites. *Compos. Struct.* **2006**, *74*, 419–425. [[CrossRef](#)]
71. Wyzgoski, M.G.; Novak, G.E. Predicting fatigue S-N (stress-number of cycles to fail) behavior of reinforced plastics using fracture mechanics theory. *J. Mater. Sci.* **2005**, *40*, 295–308. [[CrossRef](#)]
72. Paris, P.; Erdogan, F. A critical Analysis of Crack Propagation Laws. *Trans. ASME* **1963**, *85*, 528–534. [[CrossRef](#)]
73. Wyzgoski, M.G.; Novak, G.E. An improved model for predicting fatigue S-N (stress-number of cycles to fail) behavior of glass fiber reinforced plastics. *J. Mater. Sci.* **2008**, *43*, 2879–2888. [[CrossRef](#)]
74. Murakami, Y. *Stress Intensity Factors Handbook*; Pergamon Press: Oxford, UK, 1987.
75. Bond, I.P.; Ansell, M.P. Fatigue properties of jointed wood composites-Part I Statistical analysis, fatigue master curves and constant life diagrams. *J. Mater. Sci.* **1998**, *33*, 2751–2762. [[CrossRef](#)]

76. Li, Z.; Zou, H.; Dai, J.; Feng, X.; Sun, M.; Peng, L. A comparison of low-cycle fatigue behavior between the solutionized and aged Mg-3Nd-0.2Zn-0.5Zr alloys. *Mater. Sci. Eng.* **2017**, *695*, 342–349. [[CrossRef](#)]
77. Liu, Y.B.; Li, Y.D.; Li, S.X.; Yang, Z.G.; Chen, S.M.; Hui, W.J.; Weng, Y.Q. Prediction of the S–N curves of high-strength steels in the very high cycle fatigue regime. *Int. J. Fatigue* **2010**, *32*, 1351–1357. [[CrossRef](#)]



© 2018 by the authors. Licensee MDPI, Basel, Switzerland. This article is an open access article distributed under the terms and conditions of the Creative Commons Attribution (CC BY) license (<http://creativecommons.org/licenses/by/4.0/>).